New Oldowan locality Sare-Abururu (ca. 1.7 Ma) provides evidence of diverse hominin behaviors on the Homa Peninsula, Kenya

Emma M. Finestone [a,b,*], Thomas W. Plummer [c,d,e], Thomas H. Vincent [f], Scott A. Blumenthal [e,g,h], Peter W. Ditchfield [i], Laura C. Bishop [f], James S. Oliver [j], Andy I. R. Herries [k,l], Christopher Vere Palfery [k], Timothy P. Lane [m], Elizabeth McGuire [g], Jonathan S. Reeves [n,o], Angel Rodés [p,q], Elizabeth Whitfield [f], David R. Braun [n,o], Simion K. Bartilol [r], Nelson Kiprono Rotich [r,s], Jennifer A. Parkinson [e,t], Cristina Lemorini [u], Isabella Caricola [u,v], Rahab N. Kinyanjui [b,e,w], Richard Potts [e,w]

[a] Department of Anthropology, Cleveland Museum of Natural History, 1 Wade Oval Dr, Cleveland, OH, 44113, United States
[b] Department of Archaeology, Max Planck Institute for Geoanthropology, Kahlaische Str. 10, 07745, Jena, Germany
[c] Department of Anthropology, Queens College, 314 Powdermaker Hall 65-30 Kissena Boulevard Flushing, Flushing, NY, 11367, United States
[d] The CUNY Graduate Center, 365 5th Ave, New York, NY, 10016, United States
[e] Human Origins Program, National Museum of Natural History, Smithsonian Institution, P.O. Box 37012, Washington, DC, 20560, United States
[f] Research Centre in Evolutionary Anthropology and Palaeoecology, School of Biological and Environmental Sciences, Liverpool John Moores University, Byrom Street, Liverpool, L3 3AF, United Kingdom
[g] Department of Anthropology, University of Oregon, 1585 East 13th Avenue, Eugene, OR, 97403, United States
[h] Department of Earth, Ocean and Atmospheric Sciences, University of British Columbia, 2020 – 2207 Main Mall, Vancouver, BC V6T 1Z4, Canada
[i] School of Archaeology, University of Oxford, 1 S Parks Rd, Oxford, OX1 3TG, United Kingdom
[j] Anthropology Section, Illinois State Museum, 502 S Spring St, Springfield, IL, 62706, United States
[k] The Australian Archaeomagnetism Laboratory, Department Archaeology and History, La Trobe University, Melbourne Victoria, 3086, Australia
[l] Paleo-Research Institute, University of Johannesburg, 42 Bunting Rd, Cottesloe, Johannesburg, 2092, South Africa
[m] Geography and Environmental Science Research Group, School of Biological and Environmental Sciences, Liverpool John Moores University, Byrom Street, Liverpool, L3 3AF, United Kingdom
[n] Technological Origins Research Group, Max Planck Institute for Evolutionary Anthropology, Deutscher Pl. 6, 04103, Leipzig, Germany
[o] Center for the Advanced Study of Human Paleobiology, George Washington University, 800 22nd Street NW, Washington, DC, 20052, United States
[p] Departamento de Xeografía, Universidade de Santiago de Compostela, Praza da Universidade,1, 15703 Santiago de Compostela, Spain
[q] Scottish Universities Environmental Research Centre, University of Glasgow, Rankine Ave, Scottish Enterprise Technology Park, East Kilbride G75 0QF, United Kingdom
[r] Institute of Nuclear Science and Technology, University of Nairobi, P.O. Box 30197, Nairobi, Kenya
[s] Institute of Nuclear Chemistry and Technology, Dorodna 16, 03-195, Warsaw, Poland
[t] Department of Anthropology, University of San Diego, 5998 Alcala Park Way, San Diego, CA, 92110, United States
[u] LTFAPA Laboratory, Department of Science of Antiquities, Sapienza University of Rome, Piazzale Aldo Moro 5, 00185, Rome, Italy
[v] Zinman Institute of Archaeology, Haifa University, 199 Aba Hushi Avenue, Mount Carmel, Haifa, 3498838, Israel
[w] Department of Earth Sciences, National Museums of Kenya, Kipande Rd, Nairobi, Kenya

ARTICLE INFO

ABSTRACT

The Homa Peninsula, in southwestern Kenya, continues to yield insights into Oldowan hominin landscape behaviors. The Late Pliocene locality of Nyayanga (~3–2.6 Ma) preserves some of the oldest Oldowan tools. At the Early Pleistocene locality of Kanjera South (~2 Ma) toolmakers procured a diversity of raw materials from over 10 km away and strategically reduced them in a grassland-dominated ecosystem. Here, we report findings from Sare-Abururu, a younger (~1.7 Ma) Oldowan locality approximately 12 km southeast of Kanjera South and 18 km east of Nyayanga. Sare-Abururu has yielded 1754 artifacts in relatively undisturbed low-energy silts and sands. Stable isotopic analysis of pedogenic carbonates suggests that hominin activities were carried out in a grassland-dominated setting with similar vegetation structure as documented at Kanjera South. The composition of a nearby paleo-conglomerate indicates that high-quality stone raw materials were locally abundant. Tool-makers at Sare-Abururu produced angular fragments from quartz pebbles, representing a considerable contrast to

* Corresponding author.
E-mail address: efinestone@cmnh.org (E.M. Finestone).

the strategies used to reduce high quality raw materials at Kanjera South. Although lithic reduction at Sare-Abururu was technologically simple, toolmakers proficiently produced cutting edges, made few mistakes and exhibited a mastery of platform management, demonstrating that expedient technical strategies do not necessarily indicate a lack of skill or suitable raw materials. Lithic procurement and reduction patterns on the Homa Peninsula appear to reflect variation in local resource contexts rather than large-scale evolutionary changes in mobility, energy budget, or toolmaker cognition.

1. Introduction

1.1. Oldowan behavior

The appearance of stone artifacts in the fossil record represents a key behavioral innovation and adaptive shift in the human lineage (Plummer, 2004; Toth and Schick, 2018). Although the oldest stone tools (the Lomekwian) date to 3.3 Ma in West Turkana (Harmand et al., 2015), the most ancient widespread and persistent tool industry—the Oldowan—is first documented between approximately 2.9 and 2.6 Ma (Semaw et al., 1997; Braun et al., 2019; Plummer et al., 2023). The Oldowan (type site Olduvai Gorge; Leakey, 1971) was produced by striking stones to yield flakes with sharp cutting edges. Oldowan toolmakers exercised raw material selectivity and a mastery of knapping technique from the first appearance of the industry (Semaw et al., 2003; Stout et al., 2005, 2010; Rogers and Semaw, 2009; Braun et al., 2019; Plummer et al., 2023). However, variation in flaking strategy and raw material utilization has led some to note important developments in the latter half of the Oldowan Industrial Complex compared to earlier Oldowan sites (Roche et al., 2009; Goldman-Neuman and Hovers, 2012; Plummer and Finestone, 2018; Braun et al., 2019).

Oldowan sites older than 2 Ma are found in Africa primarily in paleoenvironments that span wooded grasslands and grassy woodlands in proximity to water (Quade et al., 2004; Braun et al., 2010; Cerling et al., 2011; Quinn et al., 2013; Robinson et al., 2017; Plummer et al., 2023). Artifacts at these earliest Oldowan localities are frequently in low density and lithic materials were transported over relatively short distances (generally a few tens to hundreds of meters; Harmand, 2009a, b; Rogers and Semaw, 2009; Goldman-Neuman and Hovers, 2012). The earliest sites exhibit varying degrees of technological proficiency (Kibunjia, 1994; Roche et al., 1999; Delagnes and Roche, 2005; Harmand, 2009a; Braun et al., 2019). By contrast, Oldowan sites that postdate 2 Ma are found in a broader array of paleoenvironmental settings including open grasslands and have higher artifact densities, and assemblages indicate the efficient production of stone flakes using high quality raw materials transported over much longer distances (reviewed in Braun et al., 2008a; Plummer et al., 2009b; Roche et al., 2009; Braun et al., 2010; Plummer and Finestone, 2018).

Several factors have been proposed to explain variation in tool production and utilization strategies between Oldowan sites. Variation might be attributed to sampling bias, subtle ecological differences, and/or differences in local raw material and resource availability (Semaw, 2000; Semaw et al., 2003; Braun et al., 2008c; Rogers and Semaw, 2009; Stout et al., 2010). Others have suggested that this variation might also reflect biological and behavioral changes within genus *Homo* including the expansion of diets, home ranges, manual dexterity and cognition (Rogers et al., 1994; Potts, 2007; Plummer, 2004; Plummer and Finestone, 2018). However, the taxonomic uncertainty of Oldowan toolmakers and the potential that hominin species outside of genus *Homo* made and used tools (Susman, 1988, 1991; Wood, 1997; Plummer et al., 2023) make it difficult to draw conclusions about hominin evolutionary trends from the archaeological record. A holistic understanding of Oldowan technological variability requires attention to differences in local habitat and resource availability as well as the broader environmental and evolutionary context.

The appearance and persistence of the Oldowan coincided with the turnover of multiple hominin taxa, and morphological trends such as increased body mass, cranial capacity, dental reduction and an acceleration in metabolic rate in genus *Homo* (Wrangham and Carmody, 2010; Pontzer, 2012; Antón et al., 2014). These changes may have occurred in concert with an expansion of hominin mobility, range size, and dietary breadth (Rogers et al., 1994; Antón et al., 2002; Plummer, 2004; Potts, 2007; Braun et al., 2010; Pontzer et al., 2016). Over the course of the Plio–Pleistocene, many eastern African landscapes contained significant amounts of both C_3 woody vegetation and C_4 grasses, and many mammalian herbivores ate a mix of browse and grass (Cerling et al., 2011, 2015; Levin et al., 2015; Uno et al., 2018; Polissar et al., 2019). However, the balance between C_3 and C_4 vegetation began to shift such that C_4 grasses were better represented among the range of ecosystems present across eastern Africa (Levin et al., 2015; Uno et al., 2016; Polissar et al., 2019). Although these changes might be expected to affect the spread of Oldowan technology, correlating large scale environmental shifts and hominin adaptations as a simple directional trend would ignore the climatic variability and rapid remodeling of landscapes that undoubtedly affected hominin behavior on generational timescales (Kingston, 2007; Potts and Faith, 2015). Furthermore, focusing on trends in ecological variation and hominin adaptation is complicated because the bulk of the eastern African paleoanthropological record comes from only a few basins (e.g., Turkana, Awash, Olduvai). This sample is unlikely to represent the breadth of toolmaking hominin habitats and behaviors present across space at a given time and is not at an appropriate spatial scale to capture the impact of environmental variation on the Oldowan.

Stone toolmaking is one archaeologically visible aspect of behavior that can help reconstruct hominin ecology, foraging and mobility on local and regional scales. The extent to which toolmaking behaviors varied regionally through time and according to local ecological conditions is not well understood, and site-based approaches are necessary to address this question. Here we investigate the technological strategies and ecological context at a new Oldowan locality, Sare-Abururu located on the Homa Peninsula, southwestern Kenya. We compare toolmaking strategies and local environmental conditions at Sare-Abururu with other early lithic occurrences in eastern Africa, including nearby Oldowan localities, Kanjera South and Nyayanga. We consider the extent to which Homa Peninsula tool activities reflect the local distribution of raw materials and food resources and/or long-term changes in the abilities of toolmakers through evolutionary time. If behavioral strategies on the Homa Peninsula vary primarily according to the ecological context, we expect that the Sare-Abururu artifacts will occur in localized accumulations across the landscape reflective of the local context. However, if tool assemblages reflect differences in the abilities of toolmakers related to evolutionary trends towards greater cognition, expanded range size and mobility and a shift to obligate tool use, we expect younger Oldowan assemblages to contain more sophisticated reduction sequences, longer stone resource transport distances, and denser, stratigraphically-stacked artifact accumulations compared with earlier localities on the Homa Peninsula.

1.2. Previous work on the Homa Peninsula

The Homa Peninsula, Kenya, is positioned between the two branches of the East African Rift System, on the southern margin of Lake Victoria (Fig. 1). Evidence for Oldowan hominin activities and landscape use on the Peninsula has been provided by two localities, Kanjera South and
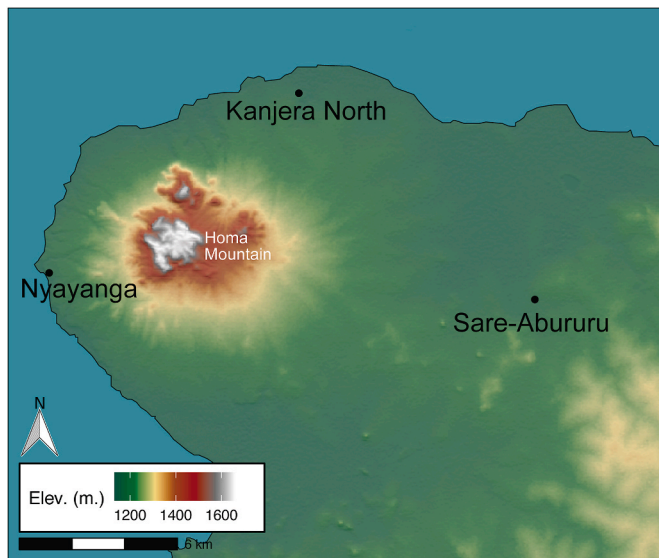
Fig. 1. The Homa Peninsula in western Kenya on the southern shores of the Kavirondo Gulf of Lake Victoria. The position of the study locality (Sare-Abururu) and Nyayanga and Kanjera South (focus of previous work) are highlighted, as well as Homa Mountain. A 30 m digital elevation model is overlaid to illustrate topographic variations across the peninsula. Digital elevation model data were accessed from the NASA Shuttle Radar Topography Mission (SRTM) Global and distributed by Open Topography.

Nyayanga. At Kanjera South (Southern Member of the Kanjera Formation), over 4400 Oldowan artifacts and thousands of faunal remains have been excavated from a 3-m-thick sequence of Early Pleistocene sediments (Behrensmeyer et al., 1995; Ditchfield et al., 1999, 2019; Plummer et al., 1999; Bishop et al., 2022). In contrast to the presence of some woody cover at many Oldowan sites, the Kanjera South paleo-ecosystem was dominated by open grassland (Plummer et al., 2009a;

Quinn et al., 2013; Plummer and Bishop, 2016).

The Kanjera South assemblage includes stone artifacts produced from diverse raw materials available on and around the Homa Peninsula (Braun et al., 2008a; Finestone et al., 2020). Hominins sometimes traveled distances over 10 km to obtain high quality 'exotic' raw materials such as quartz, quartzite, rhyolite, basalt, felsite, chert and granite (Braun et al., 2008a, 2009b; Plummer et al., 2009a; Braun and Plummer, 2013), reflecting their preference for durable materials (Braun et al., 2009a). Exotic artifacts make up a notable proportion (30%) of the assemblage, while the remaining 70% of artifacts come from local sources near the site (Braun et al., 2008a, 2009a, 2009b; Braun and Plummer, 2013).

Kanjera hominins employed different reduction strategies to maximize the number of flakes produced from exotic materials (Braun et al., 2009a; Braun and Plummer, 2013; Reeves et al., 2021). When reducing high quality cores transported from over 10 km away, hominins systematically flaked around the perimeter, exploited multiple core surfaces, maintained convex surfaces to allow longer reduction sequences, produced flakes that removed less core volume (flakes with higher edge to mass ratios) and retouched flakes. By contrast, cores from less durable local materials exhibited shorter and simpler reduction sequences with little to no retouching (Braun et al., 2009a, 2009b; Braun and Plummer, 2013). The Kanjera South artifact assemblage demonstrates that factors such as stone physical properties and raw material provenance influenced Oldowan hominin technological strategies (Reeves et al., 2021).

Kanjera South provides the earliest evidence documented so far for long-distance raw material procurement in a grassland-dominated ecosystem, indicating a potential shift towards a greater reliance on Oldowan technology and expansion into new habitats. Flakes produced from exotic raw materials were used to process a diversity of high quality, difficult to acquire foods, including animal tissue and underground storage organs (Lemorini et al., 2014, 2019). Hominins had early access to meat and focused their hunting efforts on small bovid juveniles (Plummer et al., 1999; Plummer and Bishop, 2016; Oliver et al., 2019; Parkinson et al., 2022) with a mixed strategy of hunting and scavenging
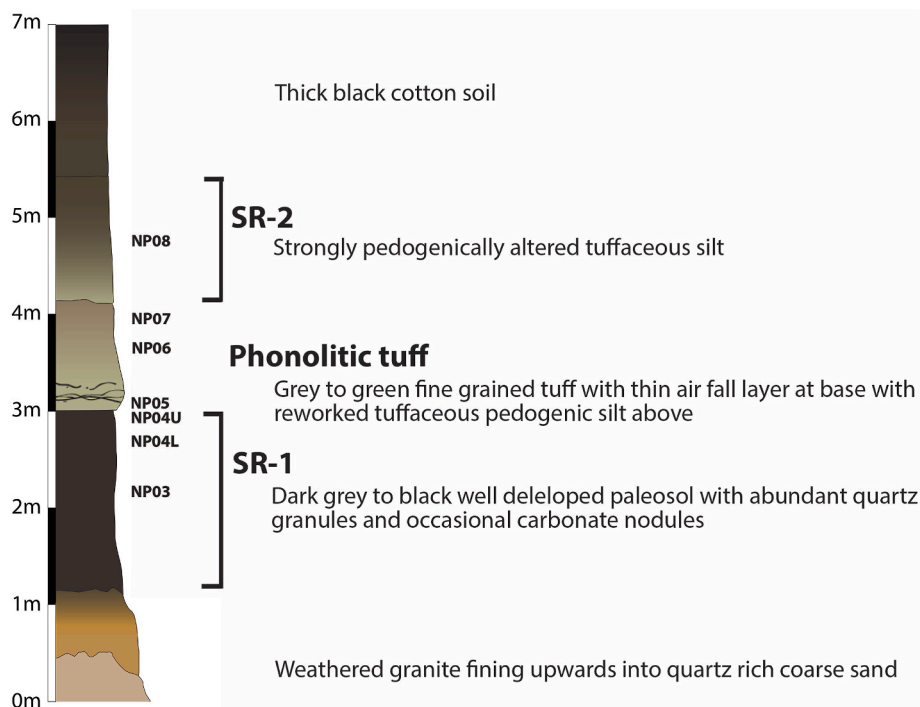

Fig. 2. Composite sedimentological log of the Sare-Abururu exposures with magnetostratigraphic sample locations (right) side by side the stratigraphy from Sare-Abururu. The two paleosol units SR-1 and SR-2 and the volcanic tuff are marked. (For interpretation of the references to color in this figure legend, the reader is referred to the Web version of this article.)
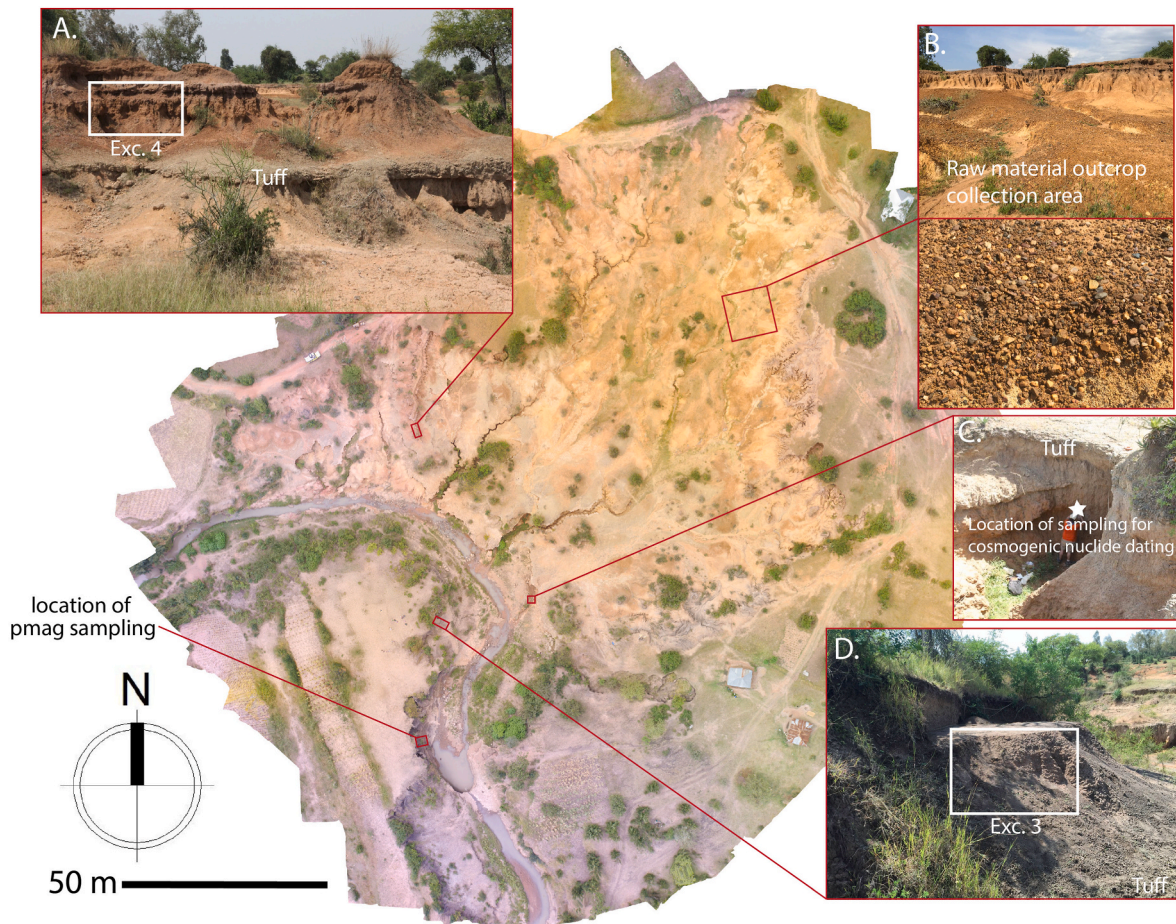
Fig. 3. Overhead view of the Sare-Abururu amphitheater with the locations of A) Excavation 4 (rectangle with underlying tuff), B) the raw material outcrop collection area, C) sampling location for cosmogenic nuclide dating (white star), and D) Excavation 3 (rectangle). The magnetostratigraphic sample location is also indicated. Excavations 1, 2 and 5 are beyond the southern margin of the figure.

individuals of larger taxa (Ferraro et al., 2013; Oliver et al., 2019).

More recently, another Homa Peninsula locality, Nyayanga, has yielded among the oldest Oldowan tools, spatially associated with *Paranthropus* remains and multiple hippopotamid butchery sites (Plummer et al., 2023). Similar to many early Oldowan localities, artifacts from Nyayanga occurred in low-density scatters along a stream channel in a wooded grassland to grassy woodland, bushland, or shrubland (Plummer et al., 2023). Hominins strategically reduced cores primarily from quartzite, quartz and rhyolite materials. Lithic use-wear revealed an emphasis on pounding behaviors, in addition to cutting and slicing activities, that were used to process a variety of plant and animal tissue. The recovery of *Paranthropus* remains alongside stone tools highlights the possibly that multiple hominin taxa may have produced and/or used early stone tools on the Homa Peninsula.

1.3. Sare-Abururu

The Sare-Abururu study locality (0°24′27.3″S, 34°37′03.1″E; Fig. 1) is located on the eastern margin of the Homa Peninsula along an alluvial plain just over 10 km from Kanjera South and 18 km from Nyayanga. The highlands to the southeast act as the primary sediment source for Sare-Abururu. This locality includes a ~15,000 m² amphitheater located on a modern river channel called the Sare River. In the amphitheater and along the river paleosols and volcanic tuff are exposed for at least 2 km and the sedimentary sequence reaches up to 7 m in thickness.

Highly weathered granite bedrock makes up the base of this sequence, which transitions into a calcareous, weathered granite fining

upward into quartz rich coarse sand. This is overlain by sedimentary unit SR-1, a 1–2-m-thick tuffaceous silt with occasional small carbonate nodules. SR-1 is capped by a grey to green fine-grained phonolitic volcanic tuff, which transitions into a 1–2-m-thick tuffaceous pedogenic silt (Unit SR-2). Sedimentary Unit SR-2, is overlain by thick black cotton soil (Fig. 2). Stone tools characteristic of the Oldowan Industry were initially observed on the surface along the Sare River.

Sare-Abururu is located near conglomerates on the eastern fringe of the Homa Peninsula, described previously in Braun et al. (2008a), that contain sources of high-quality durable lithic materials. These raw materials were exotic for hominins at Kanjera South and Nyayanga but would have been locally available to Sare-Abururu hominins. In the amphitheater, a paleoconglomerate was identified in SR-2 containing clasts of a variety of raw materials (Fig. 3).

2. Materials and methods

2.1. Excavation

In 2015, 2016 and 2017, five excavations were conducted across a 250 m transect in the tuffaceous silt. The target horizon was SR-2, the 1–2 m section of silts and sands overlaying the volcanic tuff. Each excavation proceeded in 10 cm increments (spits) within a 1 × 1 m grid until the underlying layer of tuff was reached. Excavations ranged in size from 2 m² (excavations 2, 3, 4, and 5) to 12 m² (excavation 1). Depths from the top of the excavation to the base (delineated by volcanic tuff) were 1 m (excavation 3), 1.4 m (excavation 4), 1.5 m (excavation 2), 1.6
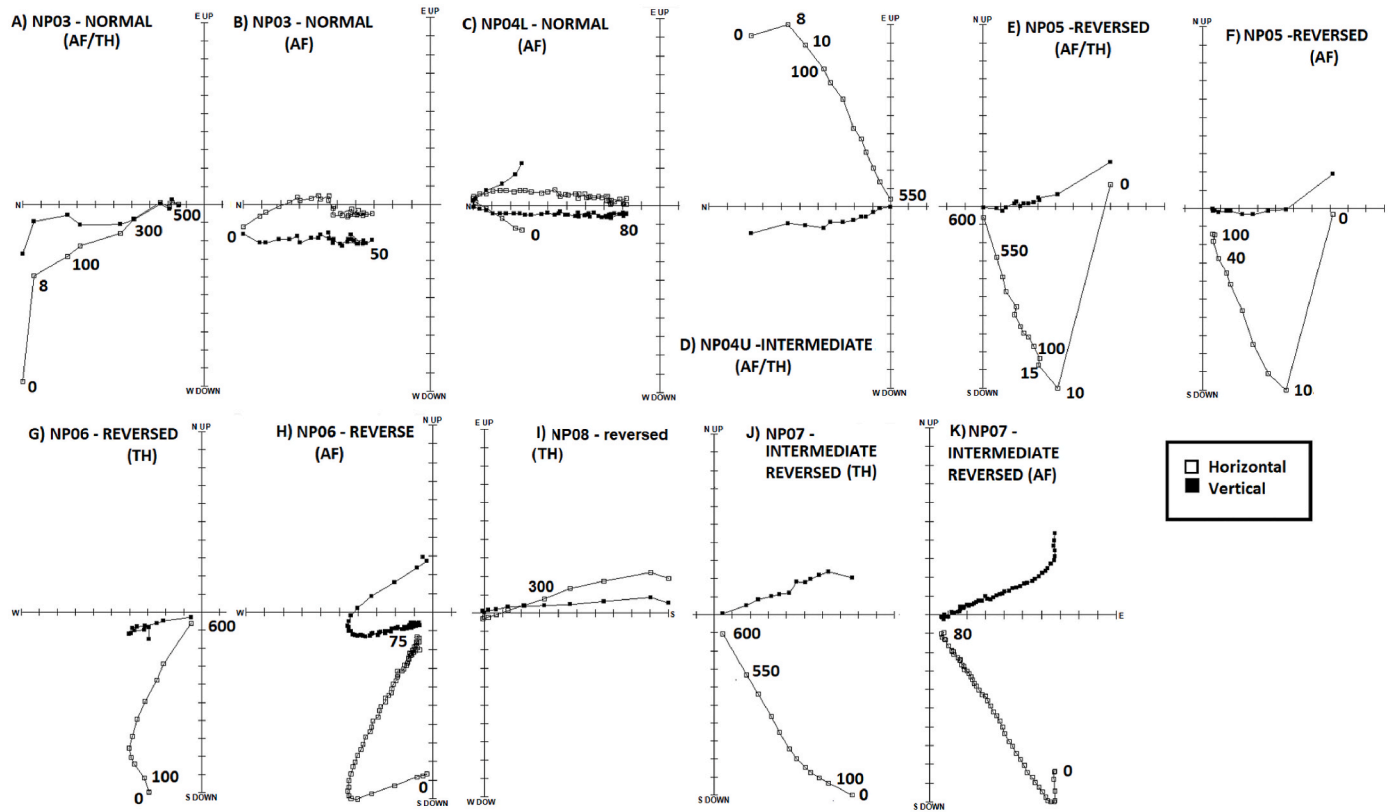
Fig. 4. Zijderveld alternating field (AF), thermal (TH) and hybrid (AF/TH) demagnetization plots for representative normal (A–C), intermediate (D), reversed (E–I) and reversed intermediate (J–K) polarity samples from Sare-Abururu. After magnetic cleaning of more recent overprints the samples all show a strong single component of magnetization that was used to resolve the final direction in individual subsamples from each level.
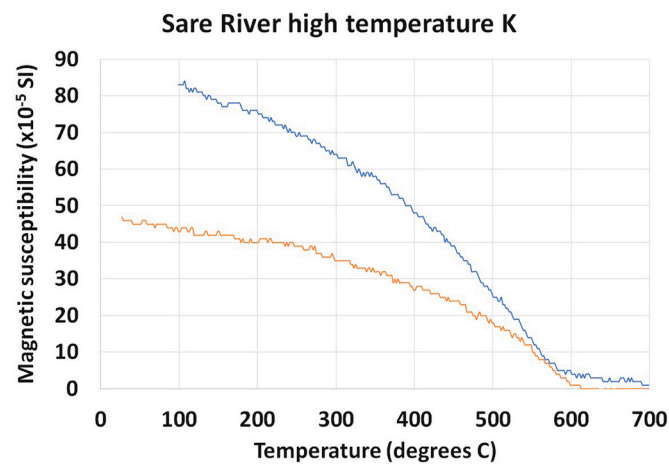

Fig. 5. High temperature magnetic susceptibility heating (orange) and cooling (blue) curves indicate that magnetite is the primary remanence carrying mineral in the Sare-Abururu samples. (For interpretation of the references to color in this figure legend, the reader is referred to the Web version of this article.)

m (excavation 1) and 1.8 m (excavation 5). All artifacts uncovered through excavation were pedestaled and a Topcon total station was used to map the position of all archaeological finds.

2.2. Chronology

Homa Peninsula geological mapping, stratigraphy and depositional history are detailed in Saggerson (1952) and Le Bas (1977). A volcanic tuff that is traceable along the Sare-Abururu area was tentatively
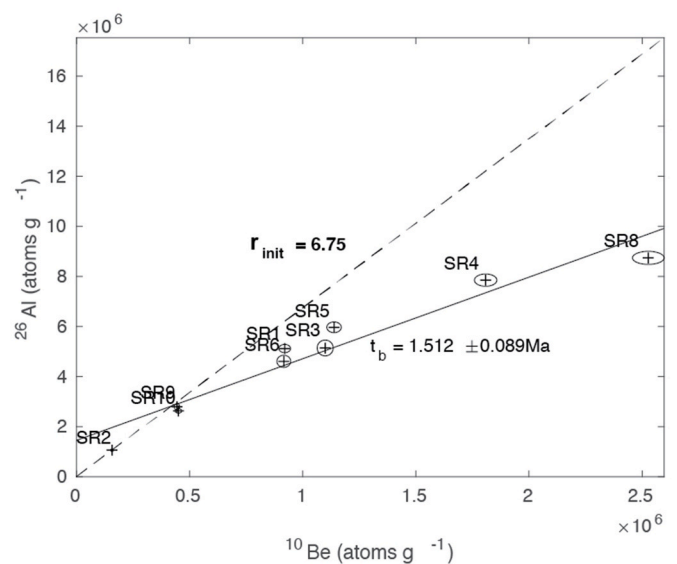

Fig. 6. Cosmogenic ^{26}Al and ^{10}Be concentrations for samples taken at Sare-Abururu. The black ellipses containing plus signs represent the uncertainties in the concentrations. The dashed line displays the production ratio $P_{26}(0)/P_{10}(0)$ for comparison. The solid line is the best fit to the ^{26}Al and ^{10}Be data, on which all samples lie. This indicates that samples are consistent with a single age of deposition at 1.512 ± 0.089 Ma.

identified as the 'Orio tuff.' The Orio tuff was suggested to coincide with Late Pliocene/Early Pleistocene volcanic activity that occurred peripherally to the Homa Mountain carbonatite complex (Le Bas, 1977).
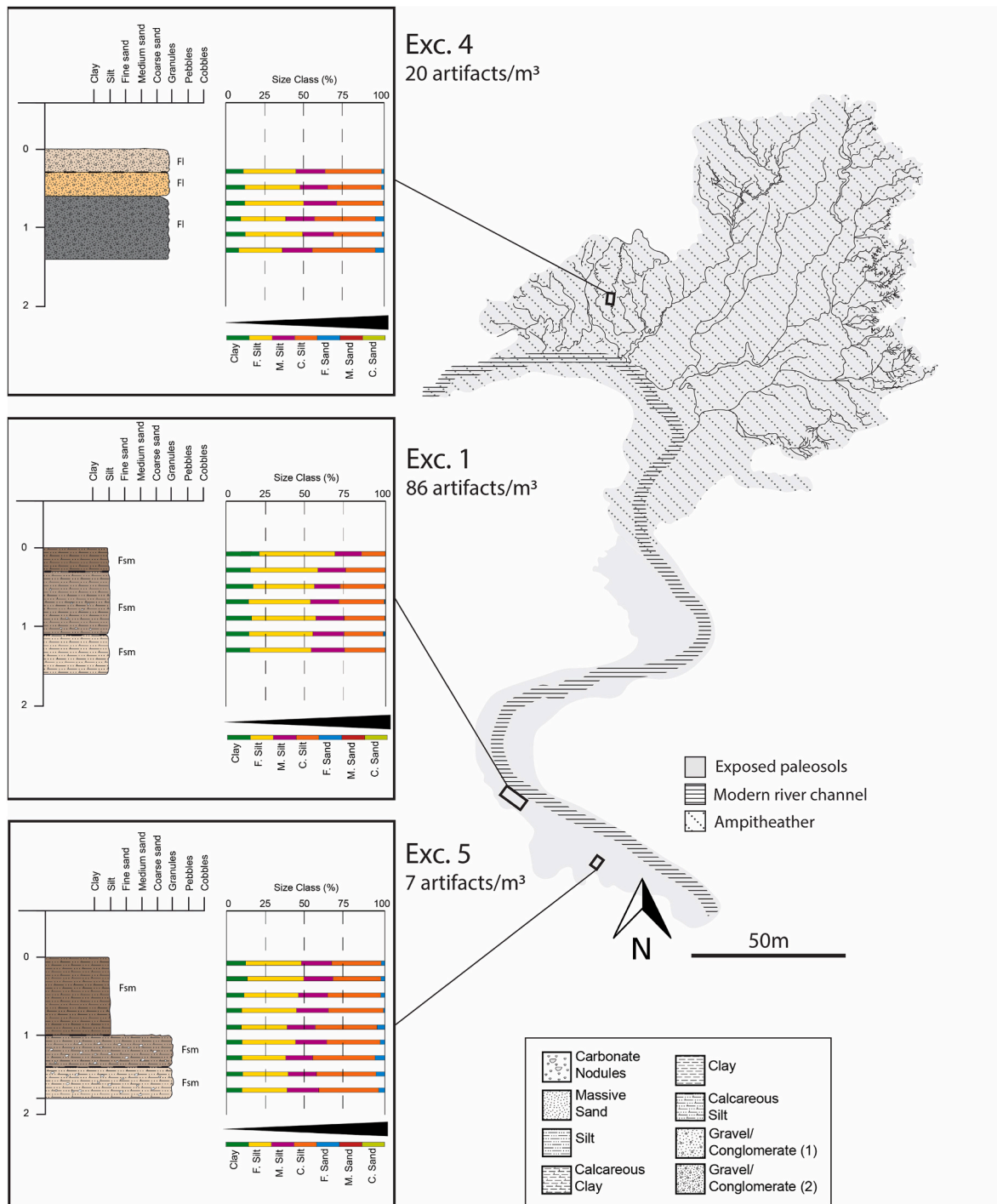
Fig. 7. Sediment log of excavations 4, 1 and 5 at Sare-Abururu. Sediment log depth is in meters. Facies codes outlined by Miall (2013) are included on sediment logs. Particle size distributions are also included at corresponding sample depths.

Electron microprobe analysis of the glass fraction of the Sare-Abururu tuff indicates that the tuff is phonolitic, confirming that it is not derived from the Homa Mountain carbonatite complex. Attempts to use Ar^{40}/Ar^{39} radiometric methods to provide an age estimation of the tuff failed. Multiple samples did not yield feldspathic or biotite crystals amenable to radiometric methods (S. Nomade, personal communication, 2/13/2020). However, the Nyamatoto phonolite plug adjacent to Homa Mountain is a prominent source of phonolite volcanism in the area. The emplacement phase of this edifice has a whole rock K/Ar date of 1.73 ± 0.06 Ma (Le Bas, 1977). This is the likely source of the tuffaceous material dubbed the 'Orio Tuff,' in which case we expect that

SR-1 and SR-2, which bracket the tuff, would have been deposited just before and after that date, respectively. This interpretation is consistent with the depositional sequence of Homa Peninsula sediments described by Le Bas (1977). Here we utilize magnetostratigraphy and cosmogenic nuclide dating to provide further evidence for the age of the Sare-Abururu sequence.

Magnetostratigraphy Samples for paleomagnetic analysis were collected as oriented block samples from seven levels through the paleosol and tuff sequence at the location indicated in Figure 2. They were cut into at least three standard paleomagnetic cubes per layer for the laboratory analysis. The block samples were then cut into standard 2.5 cm² cubes in

Table 1
Stable carbon and oxygen isotopic composition of pedogenic carbonates.

Sample ID	Geotrench/excavation	Unit	$\delta^{13}C$	$\delta^{18}O$
SBK-16C-1	2016-2A	SR-2	−0.3	−4.3
SBK-16C-2	2016-2A	SR-2	−2.6	−6.9
SBK-16C-3	2016–3	SR-2	0.5	−2.8
SBK-16C-4	2016–4	SR-2	−1.0	−2.7
HOM20-01	Section Hom-20	SR-1	−8.9	−1.5
HOM20-02	Section Hom-20	SR-1	−7.8	1.2
HOM20-03	Section Hom-20	SR-1	−8.4	−1.8
HOM19-01	Section Hom-19	SR-2	−2.4	−0.1
HOM19-02	Section Hom-19	SR-2	−1.3	−2.3
HOM19-03	Section Hom-19	SR-1	−3.5	−0.2
HOM19-04	Section Hom-19	SR-1	−2.2	−0.7
HOM19-05	Section Hom-19	SR-1	−3.1	−1.4
EX1-50	Exc 1	SR-2	−1.0	−2.5
EX1-80	Exc 1	SR-2	−1.0	−1.9
EX2-TOP	Exc 2	SR-2	−0.8	−2.1
EX2-Base	Exc 2	SR-2	−1.8	−4.7
EX5-0	Exc 5	SR-2	−0.9	−2.7
EX5-60	Exc 5	SR-2	−1.6	−3.1
EX5-100	Exc 5	SR-2	−1.1	−2.9
EX5-160	Exc 5	SR-2	0.2	−1.5
EX5-170	Exc 5	SR-2	1.0	−2.3

Exc = excavation.

Table 2
Stable carbon isotopic composition of the bulk organic matter within top 15 cm of the SR-1 paleosol.

Sample ID	$\delta^{13}C_{VPDB}$	%C
SR14-1	−13.59	0.12
SR14-5	−14.96	0.12
SR14-6	−12.97	0.11
SR14-7	−14.94	0.14
SR14-17	−13.56	0.07
SR14-18	−13.95	0.06
SR14-19	−13.80	0.07
SR14-20	−14.30	0.07
SR14-21	−14.89	0.09
SR14-22	−12.72	0.12

the laboratory. Following Herries et al. (2020), sub-samples from each of these layers were subjected to a range of magnetic cleaning strategies including alternating field (AF), thermal (TH) and a hybrid AF/TH demagnetization. All samples were measured on an AGICO JR6 spinner magnetometer within a magnetic measurements shielded room. Some specimens were demagnetized using a laboratory-built AF demagnetizer equipped with a sample tumbler and Helmholtz coils to minimize the ambient field, capable of imparting fields of up to 100 mT. A later batch of samples was demagnetized using an AGICO LDA5 AF demagnetizer capable of imparting fields up to 200 mT. Thermal demagnetization was conducted using a Magnetic Measurements MMTD80 Thermal Demagnetizer. Stable characteristic remanent magnetization (ChRM) directions were determined using principal component analysis (Kirschvink, 1980) with accepted samples having a Maximum Angular Deviation <10°. Final mean directions, K (Fisher, 1953) and paleolatitudes were calculated for each block sample (layer) using the program FISH2 v. 2 (Liverpool, UK). Normal and reversed polarities were determined by positive or negative values > 60°, with values below 45° defined as intermediate. Between 60° and 45° they were defined as intermediate normal or reversed.

Cosmogenic nuclide dating The use of cosmogenic nuclide dating has become increasingly common in archaeological contexts, providing relatively accurate, precise and independent dates up to ca. 5 Ma (Granger and Muzikar, 2001; Gibbon et al., 2014; Granger, 2014; Çiner et al., 2015; Granger et al., 2015; Liu et al., 2015). This technique was implemented to constrain the age of archaeological occurrences and act as an independent chronological control for other dating methods

utilized on the Homa Peninsula.

The isochron burial method was applied (Balco and Rovey, 2008; Supplementary Online Materials [SOM] S1). Nine samples were collected from unit SR-1 using a stainless-steel trowel from conglomerate deposits thought to have been rapidly buried in the main Sare-Abururu amphitheater (Fig. 3). Samples included one sample of ca. 60 quartzite pebbles, two samples of sand and six individual clasts. All samples (SR1–SR9) were acquired from the same location in the lower meter of a single 3–4 m thick facies of fluvial sands and gravels. The sampled facies were at the base of a 5.1 m section situated above a highly weathered granite bedrock, and below a 3–50 cm tuff layer (location in Fig. 3C). All samples were collected from deposits that had been buried under at least 3 m of sediment to ensure burial and isotopic decay as suggested by Granger (2014).

2.3. Reconstructing environmental context

Sedimentology Sediment spot samples were taken from excavations 1, 4 and 5. The weathering profile was removed from the face of the exposure prior to sampling and then the sediment was collected using a clean stainless-steel trowel. The classification system proposed by Miall (SOM Table S1) was used to provide a basis for identifying lithofacies locality wide and adhere to a standardized classification system (Miall, 2013). Observations were made on color, composition, particle size and sedimentary structures. After their removal, carbonate nodules were inspected with a hand lens and the presence of coalescing carbonates and carbonate horizons was noted. Samples were taken from each of the lithofacies identified, as well as at varying lateral locations. Assessments of both the paleo- and modern geomorphological profile were made. This information was used to develop and refine a facies model, which divides the sequence into different lithofacies.

Field observations of sediments provide a partial understanding of the depositonal history of the Sare-Abururu deposits. Particle size analysis (PSA) of the fine fraction in the laboratory provided more clarity about the sedimentary processes occurring at Sare-Abururu. Particle size was measured using laser diffraction (SOM S2). The technique is based on the light diffraction theory that particles of given sizes diffract light at certain angles while passing through a sample cell in suspension. The diffracted light intensity is then measured by detectors (which measure volume percentage) and measurements are processed using one of two diffraction models (Mie theory or the Fraunhofer theory; Beuselinck et al., 1998). In this study, a Beckman Coulter LS11320 laser granulometer was used to measure particle size using the Fraunhofer model (SOM S2).

Stable isotopes of pedogenic carbonates and organic matter The stable isotopic composition of paleosol organic matter and pedogenic carbonates relates to the isotopic composition of overlying vegetation during the period of soil and carbonate formation and has been widely used to reconstruct past environments in Africa (Sikes, 1994; Plummer et al., 2009b; Cerling et al., 2011). In areas where C_4 plants are present, the carbon isotopic composition of soil organic matter and soil carbonates reflects the fraction of C_4 plants vs the fraction of C_3 woody cover. Thus, paleosol stable isotopic composition can distinguish among the following vegetation structure categories defined as the percentage of woody cover: grasslands (0–10%), open wooded grasslands (10–20%), wooded grasslands (20–40%), grassy woodlands/bushlands/shrublands (40–60%), woodlands/bushlands/shrublands (60–80%) and forests (80–100%; Cerling et al., 2011, 2013). In this study, stable isotope analysis was performed on pedogenic carbonates and organic matter preserved in bulk paleosol samples.

Pedogenic carbonates were analyzed from units SR-1 and SR-2. Six pedogenic carbonates were collected from sediments in unit SR-1 and 15 pedogenic carbonates were collected from excavations 1, 2, 3, 4 and 5 and surrounding areas in unit SR-2. Pedogenic carbonates were all either nodular or rhizoliths and exhibited micritic microstructure consistent with in situ formation (no coarser grained sparry cements were observed). Prior to analysis, the carbonate samples were washed in
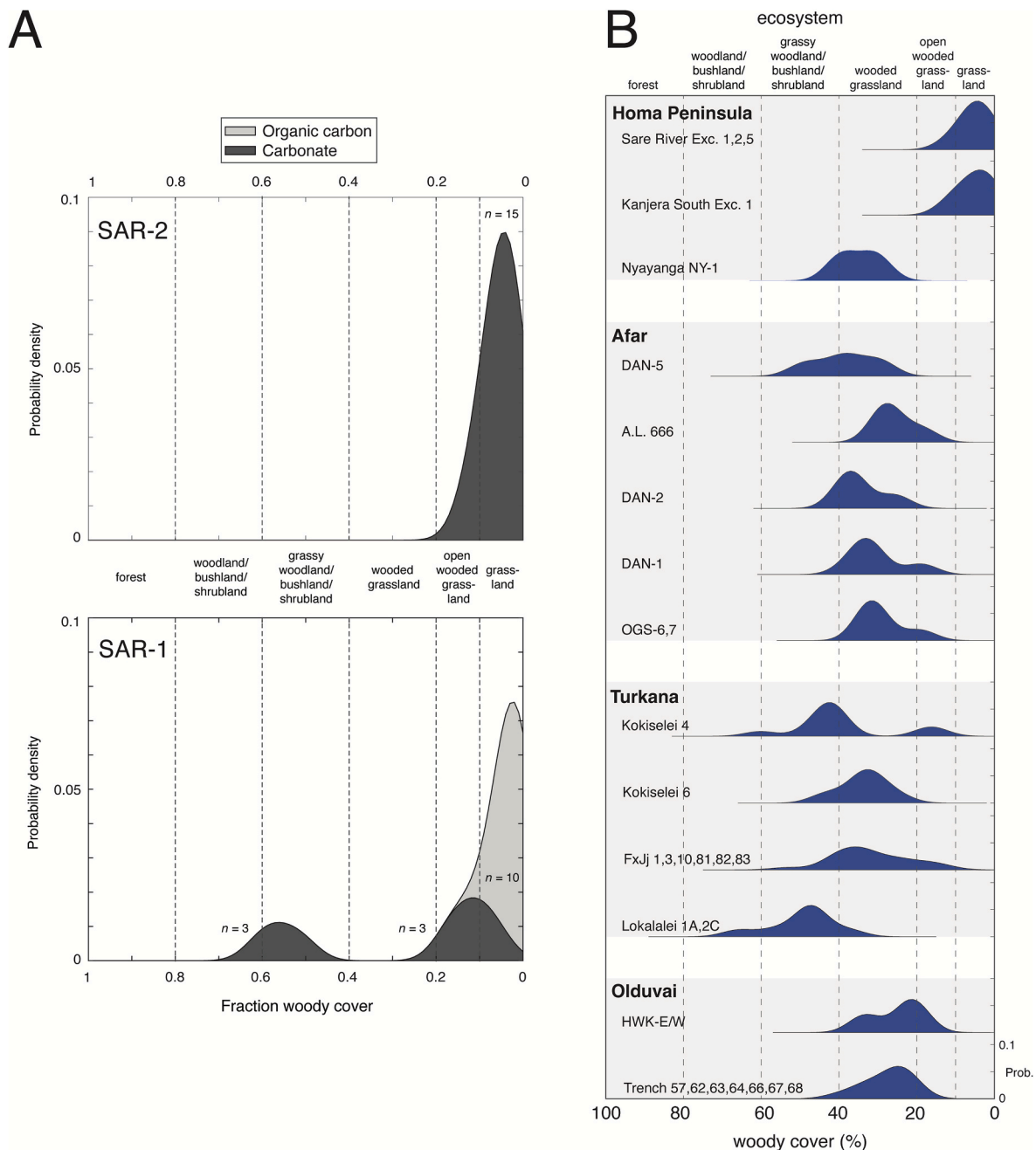
Fig. 8. A) Modeled woody cover based on $\delta^{13}C$ from pedogenic carbonates and bulk organic matter samples collected below (SR-1) and above (SR-2) the phonolitic tuff. B) Modeled woody cover from Sare-Abururu excavations compared to other Early Stone Age lithic sites in eastern Africa from ca. 2.6–1.5 Ma. The compilation only includes pedogenic carbonates collected in association (i.e., close in space and stratigraphy) with archaeological levels (SOM Table 7; Sikes, 1994; Plummer et al., 1999, 2009, 2023; Levin et al., 2004, 2011; Sikes and Ashley, 2007; Aronson et al., 2008; Cerling et al., 2011; Quinn et al., 2013).

deionized water and dried. The outer layers of the carbonate nodules were removed using a dental burr and discarded. The inner part of each carbonate nodule was crushed in an agate mortar and each sample was split into two aliquots. The first aliquot, for analysis of carbonate, was treated with 2% NaOHCl solution at 60 °C for 24 h to remove any organic contamination. Carbonate samples were analyzed using a microCAPS unit by reacting with 100% phosphoric acid at 90 °C and analyzing resulting CO_2 using a Sercon Geo 20–22 IRMS. After analysis of carbonate samples, results are normalized to the VPDB scale using IAEA–CO–1, NBS-18 and NBS-19 where repeat analysis indicates reproducibility is ±0.1‰ (1σ) or better.

Paleosol samples for bulk organic carbon analysis were collected along a ~150 m transect along the modern river channel near the

amphitheater in areas where the paleosol horizon underlying the tuff is well developed and clearly exposed, near excavation 3, excavation 4 and the cosmogenic nuclide dating sampling site. Samples were collected using metal tools from shallow trenches dug in the top 15 cm of the paleosol horizon. At two locations, samples were also collected at greater depths at 15 cm increments to a maximum of 90 cm. Samples were air dried in the field. Prior to analysis, each sample was reacted with 0.5 M HCl for 24 h to remove carbonates, rinsed (5×) using ultra-pure (Type 1) water and dried at 60 °C for 48 h. The carbon isotope composition of bulk organic matter was determined by combusting samples using a EuroVector elemental analyzer and measuring $^{13}C/^{12}C$ ratios of the resulting gas using a Nu Horizon II gas source isotope ratio mass spectrometer at the University of Oregon. Analytical
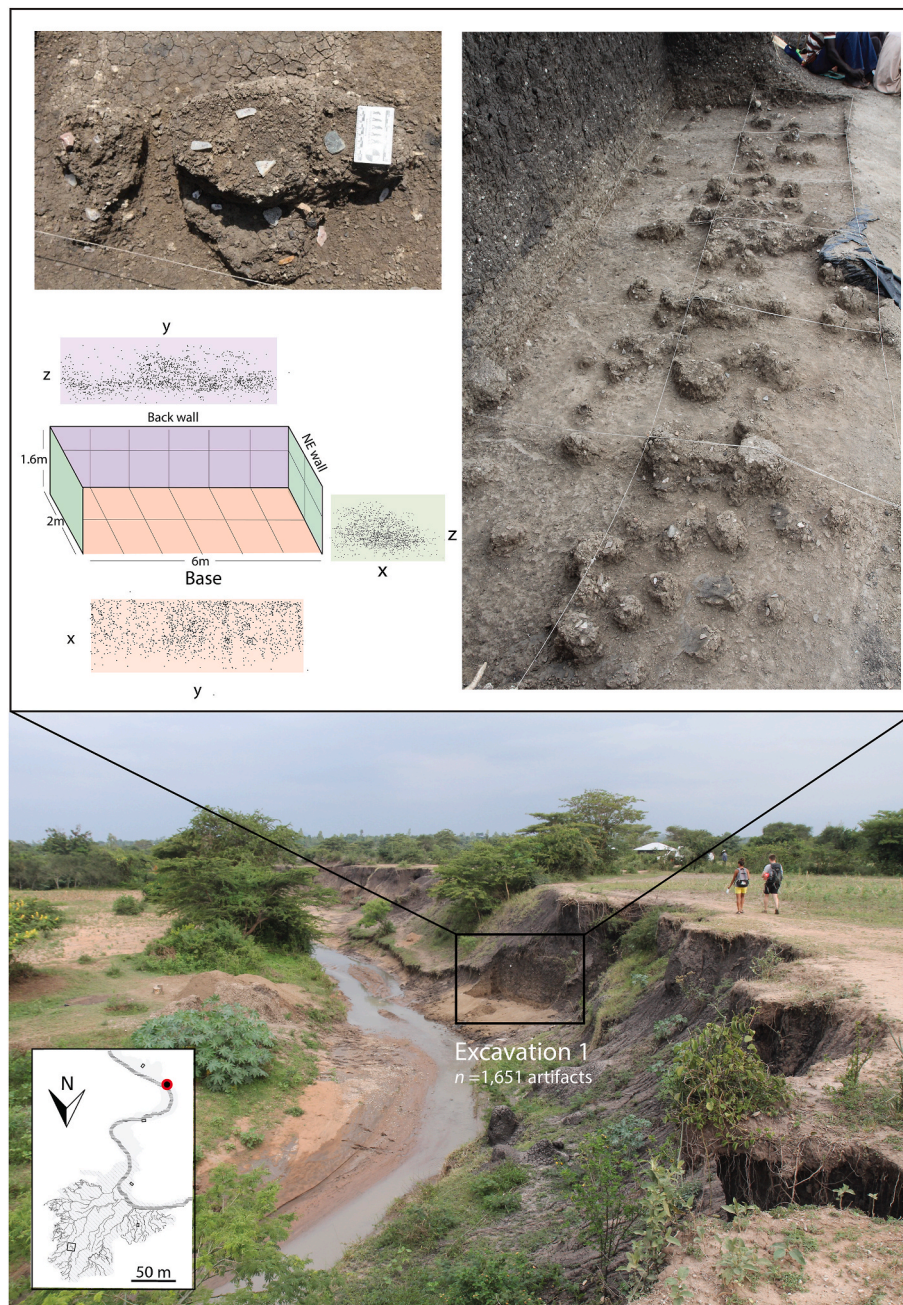
Fig. 9. Photos of excavation 1 excavation area with schematics of the excavation dimensions and projected artifact scatters in two dimensions. Each dot represents an artifact.

reproducibility was assessed by repeated analyses of wheat ($\pm0.1‰$, 1σ) and sorghum ($\pm0.4‰$, 1σ) standards.

All isotopic results are reported using the conventional δ-notation relative to internationally accepted VPDB (Vienna PeeDee Belemnite), where $\delta^{13}C = (R_{sample}/R_{standard} - 1) \times 1000$ and R_{sample} and $R_{standard}$ are the $^{13}C/^{12}C$ ratios of the sample and standard, respectively.

Following Cerling et al. (2011), we estimated percent woody cover from the carbon isotope composition of Sare-Abururu pedogenic carbonate and paleosol bulk organic matter samples. In addition, we model woody cover for other Early Stone Age archaeological sites in eastern Africa ranging in age from ~2.6 Ma to ~1.6 Ma using previously published $\delta^{13}C$ values from pedogenic carbonates sampled within or near lithic sites (Sikes, 1994; Plummer et al., 1999, 2009b, 2023; Levin et al., 2004, 2011; Sikes and Ashley, 2007; Aronson et al., 2008; Cerling et al., 2011; Quinn et al., 2013).

2.4. Lithic analysis

All lithics recovered through excavation were analyzed. Artifacts were categorized as detached pieces, pounded pieces, or flaked pieces (Isaac et al., 1997). Detached pieces were further classified into debitage types (whole flakes, broken flakes, or angular fragments). Each artifact was weighed using a digital scale to 0.1 g and the maximum dimension, measured as the longest distance across an artifact, was recorded (Andrefsky, 1998). Maximum dimension and all other linear dimensions were measured in millimeters using digital calipers to the nearest 0.1 mm. The lithic assemblage at Sare-Abururu is overwhelmingly dominated by detached pieces. As a result, our analysis primarily focused on flake attributes.

Flake attributes Flake length was defined as the distance between the point of initiation to the distal end of the flake on the ventral surface in
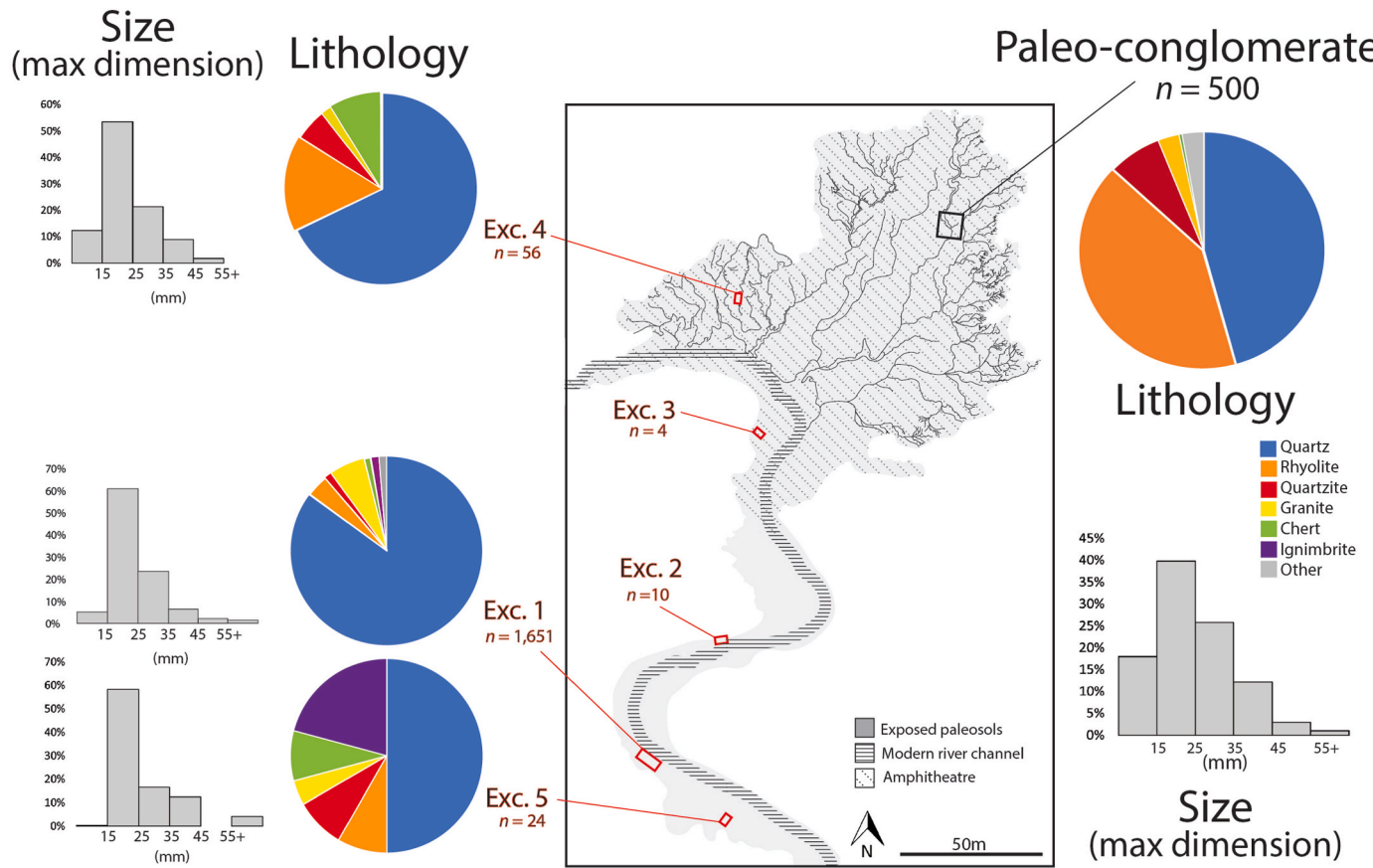
Fig. 10. The composition of artifacts from excavations 1–5 in terms of raw material type (lithology) and size (maximum dimension of piece) compared to the composition of available clasts in the paleo-conglomerate. (For interpretation of the references to color in this figure legend, the reader is referred to the Web version of this article.)

Table 3

The observed counts of raw materials in the artifact assemblage versus the expected counts of raw materials. Standardized residuals are also reported. The difference between observed and expected counts are significant ($\chi^2 = 813.3$, $p < 0.001$).

	Observed	Expected	Standardized residuals
Quartz	1471	801	23.7
Granite	102	49	7.6
Rhyolite	72	724	−24.2
Quartzite	33	123	−8.1
Chert	25	7	6.8

the direction of percussion (Debénath and Dibble, 1994). The width was measured as the distance across the ventral surface of the flake at the midpoint, perpendicular to the axis of technological length. Thickness was measured at the axis perpendicular to width and length. The type of fracture termination was recorded as feather, step, hinge, or overshot.

Attributes of the dorsal surface, such as cortex and characterization of flake scars, were noted. Flake scars were defined as the negative impressions made from previous removals with a maximum dimension greater than 10 mm. The number, direction and termination of dorsal flake scars were recorded. The dorsal cortex is an estimation of the percentage of cortex on the dorsal surface. Here it was estimated using an eight-stage system previously employed by Roth and Dibble (1998) and Braun et al., (2008d). This system assigns a number 1–8 based on the degree of remnant cortex present (8 = 0%; 7 = 1–10%; 6 = 11–30%; 5 = 31–50%; 4 = 51–70%; 3 = 71–90%; 2 = 91–99%; 1 = 100%). The termination type of flake scars was also categorized as feather, step, hinge, or overshot.

The number of platform facets and the amount of platform cortex were also recorded. Platform facets indicate that previous removal surfaces were used to generate subsequent flake removals and are indicative of bifacial or multifacial reduction. The amount of platform cortex was estimated in 10% intervals (e.g., 0, 1–10%, 10–20%, etc.). Platform thickness was defined as the distance across the platform between the ventral and the dorsal margin at the point of initiation of percussion. Length was defined as the distance of a line perpendicular to the midpoint of platform thickness.

Flakes were classified into Toth's Technological Flake Categories I–VI (Toth, 1982; SOM S3) based on the presence or absence of cortex on the dorsal surface and platform. Technological Flake Categories offer a measure of reduction intensity (Kimura, 1999, 2002; de la Torre et al., 2003), assemblage integrity and degree of transport (Schick, 1987; Stout et al., 2010). Prevalence of Toth Types I–III is associated with early stage flaking and is often indicative of unifacial reduction, while later stage Technological Flake Categories represent a higher degree of reduction intensity and bifacial reduction (Toth, 1987; Stout et al., 2010).

The simplicity of Technological Flake Categories makes it a useful system that can be applied to many Oldowan assemblages. However, this system is heavily influenced by initial clast size, such that larger cores are significantly associated with lower frequencies of Toth Types I–III (Toth, 1997; Braun et al., 2008d). An alternate method for reconstructing the reduction sequence in Oldowan assemblages is Braun et al.'s (2008b) multiple linear regression model that incorporates several other variables to more accurately predict a flake's position in the reduction sequence. The formula for the stepwise multiple linear regression model with the lowest standard error of estimate applicable to Oldowan flaking is:

Table 4
Weight and maximum dimensions of artifacts in the Sare-Abururu assemblage. Count, percent, maximum dimension and width are reported for each artifact type and raw materials in Excavations 1, 2, 3, 4 and 5.

Excavation	Technological category	Raw material	n	%	Max dim (mm)		Weight (g)	
					Mean	Std dev	Mean	Std dev
Exc 1 (n = 1651)	FP	Quartz	3	0.2	30.5	4.8	16.0	7.8
		Quartzite	1	0.1	63.3	–	99.5	–
		Rhyolite	1	0.1	44.4	–	36.6	–
		Granite	2	0.1	72.5	6.3	179.3	123.2
		Chert	0	0.0	–	–	–	–
		Ignimbrite	0	0.0	–	–	–	–
		Total	7	0.4	49.2	20.2	77.9	90.6
	DP	Quartz	1403	85.0	24.4	54.0	3.2	9.0
		Quartzite	27	1.6	33.7	15.6	12.1	15.9
		Rhyolite	60	3.6	24.5	9.5	4.0	8.6
		Granite	97	5.9	34.9	14.7	12.8	20.5
		Chert	16	1.0	24	6.2	2.6	1.7
		Ignimbrite	22	1.3	32	17.7	14.4	29.4
		Total	1644	99.6	25.3	50.2	4.2	11
	PP	–	0	0.0	–	–	–	–
Exc 2 (n = 10)	FP	–	0	0.0	–	–	–	–
	DP	Quartz	8	80.0	27.3	16.8	6.0	8.3
		Quartzite	0	0.0	–	–	–	–
		Rhyolite	0	0.0	–	–	–	–
		Granite	0	0.0	–	–	–	–
		Chert	2	20.0	22.4	3.6	2.14	0.6
		Ignimbrite	0	0.0	–	–	–	–
		Total	10	100.0	26.3	15.0	5.2	7.5
	PP	–	0	0.0	–	–	–	–
Exc 3 (n = 4)	FP	–	0	0.0	–	–	–	–
	DP	Quartz	2	50.0	16.4	3.5	0.8	0.6
		Quartzite	0	0.0	–	–	–	–
		Rhyolite	0	0.0	–	–	–	–
		Granite	0	0.0	–	–	–	–
		Chert	0	0.0	–	–	–	–
		Ignimbrite	1	25.0	39.7	–	26.9	–
		Total	4	100.0	20.8	13.0	7.2	13.2
	PP	–	0	0.0	–	–	–	–
Exc 4 (n = 56)	FP	Quartz	1	1.8	38.7	–	11.6	–
		Quartzite	0	0.0	–	–	–	–
		Rhyolite	1	1.8	48.0	–	45.5	–
		Granite	0	0.0	–	–	–	–
		Chert	0	0.0	–	–	–	–
		Ignimbrite	0	0.0	–	–	–	–
		Total	2	3.6	43.3	6.6	28.4	24.2
	DP	Quartz	37	66.1	20.9	6.9	1.9	2.2
		Quartzite	3	5.4	24.5	9.1	3.2	3.2
		Rhyolite	8	14.3	27.4	8.7	5.5	5.8
		Granite	1	1.8	23.2	–	1.4	–
		Chert	5	8.9	21.3	8.0	1.3	1.5
		Ignimbrite	0	0.0	–	–	–	–
		Total	54	96.4	22.1	7.4	2.4	3.1
	PP	–	0	0.0	–	–	–	–
Exc 5 (n = 24)	FP	–	0	0.0	–	–	–	–
	DP	Quartz	17	70.8	23.7	9.2	5.2	6.6
		Quartzite	2	8.3	23.4	2.1	3.4	1.5
		Rhyolite	2	8.3	27.8	10.5	5.3	6.4
		Granite	1	4.2	96.1	–	92.2	–
		Chert	2	8.3	25.3	8.6	5.7	5.6
		Ignimbrite	0	0.0	–	–	–	–
		Total	24	100.0	27.2	16.8	8.7	18.7
	PP	–	0	0.0	–	–	–	–

Abbreviations: Max dim = maximum dimension; Std dev = standard deviation; Exc = excavation; FP = flaked piece; DP = detached piece; PP = pounded piece.

$$\sqrt{\text{Flake sequence number}} = [(\text{Flake scar direction} \times 0.628) + (\text{Platform facets} \times 1.008) + (\text{Flake scar}/\log_{10} (\text{Flake length} \times \text{Flake width}) \times 0.159) + (\text{Dorsal cortex}/\log_{10} (\text{Flake length} \times \text{Flake width}) \times 0.097)] \quad \text{(formula 1)}$$

This formula was used to reconstruct a flake's stage in the reduction sequence.

Finally, the ratio of flake edge to mass is relevant in reconstructing flake efficiency and raw material conservation (Braun and Harris, 2003). The ratio of edge length (cm)/$\log_{10}$ (mass) provides a measure of flake utility and an estimate of the amount of cutting edge produced from a given quantity of stone (Braun, 2005; Braun and Harris, 2003; Mackay, 2008). Edge length can be directly measured from the flake or from image analysis (Braun and Harris, 2003). Mackay (2008) has demonstrated that edge length can also be reliably estimated from flake dimensions. The formula for estimating edge length is:

$$\text{Edge length} = \text{Maximum width} + \text{Technological length} + \text{Maximum dimension} \quad \text{(formula 2)}$$

Core attributes Maximum core length was measured as the longest axis of the cobble. Core width was measured perpendicular to the axis of maximum length. Core thickness was measured as the maximum
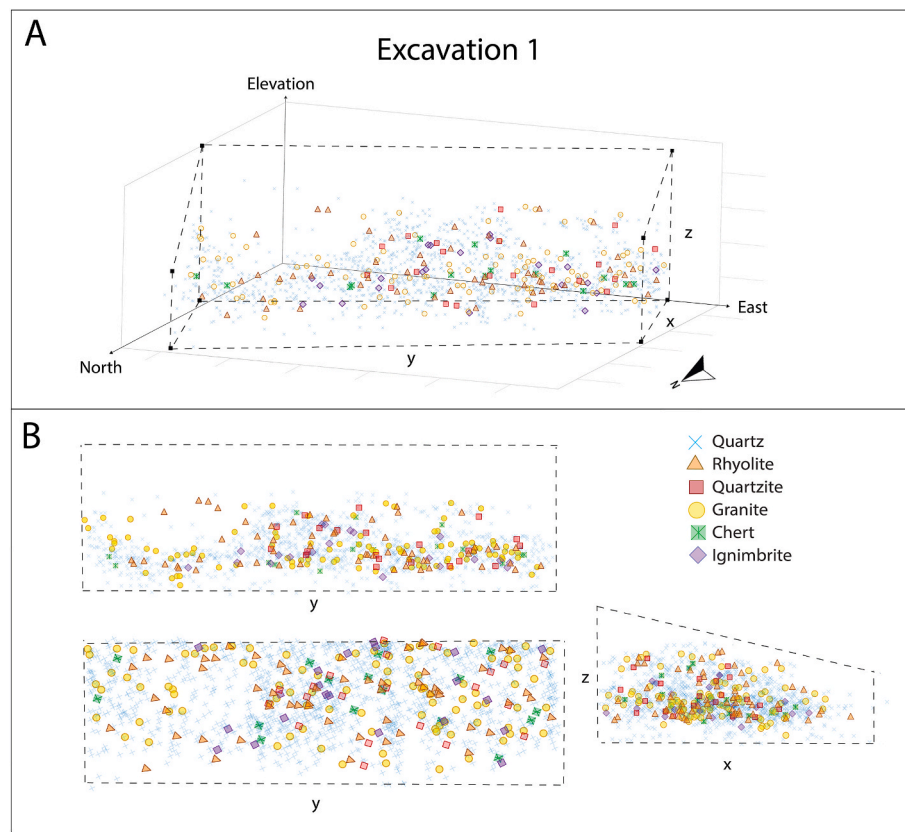
Fig. 11. The distribution of stone tools in excavation 1 according to raw material type. Each data point represents a stone tool, with symbols and colors representing raw material type (quartz, rhyolite, quartzite, granite, chert and ignimbrite). Four views of excavation 1 are presented: A three-dimensional view (A) and two-dimensional views (B) from the perspective of overhead (x, y), front (y,z) and side (x, z). (For interpretation of the references to color in this figure legend, the reader is referred to the Web version of this article.)

dimension that is perpendicular to the axis of length and the axis of width. Core percent cortex was used as an estimate of the amount of cortex covering the whole piece and was estimated within 10%. Negative flake scars on the surface of the core were counted.

Raw materials The frequency of different rock types was determined in the artifact assemblage and in the nearest outcropping conglomerate located in unit SR-2 within the amphitheater (Fig. 3). A random sample of 500 cobbles was collected from a 2 m^2 section of the conglomerate. All artifact and conglomerate samples were attributed to lithological groups through visual inspection with a 10 × hand lens and maximum dimension was recorded.

2.5. Statistical comparisons

To investigate the lithic technology at Sare-Abururu with respect to other archaeological assemblages, we compared technological measurements using a principal component analysis (PCA). Previous studies have used PCA to distinguish industries and compare Early Stone Age assemblages (Braun et al., 2019; Mercader et al., 2021; Plummer et al., 2023). Here we compared Sare-Abururu with technological attributes from Oldowan and Acheulean assemblages compiled in previous studies (Braun et al., 2019; Mercader et al., 2021; Plummer et al., 2023). The technological variables included in the PCA were: percentage of cores in the assemblage, percentage of angular fragments relative to detached pieces in the assemblage, average core maximum dimension, the ratio of average flake size to average core size, average flake scar count, the ratio of flake scar count to the log of mean core size, average flake maximum dimension, average flake thickness and the percentage of the assemblage that had

evidence of percussion. These technological variables were defined and calculated according to Braun et al. (2019). Assemblages with missing data were omitted from the analysis. The resulting dataset underwent a PCA based on a correlation matrix in the statistical software R v. 4.2.2 (R Core Team, 2022) using the FactoMineR package (Lê et al., 2008).

To test whether the rock types present in the artifact assemblage reflected local lithologies, we calculated expected raw material counts based on the frequency of raw materials in the local conglomerate. These counts were compared with the observed count of raw materials in the artifact assemblage. A Chi-squared test was used to assess this difference. We also performed a linear regression on the average carbon isotopic composition (dependent variable) and the average carbon contents of paleosol bulk organic matter. For all statistical tests, significant differences were determined using an alpha level of 0.05 and all statistical tests were performed in R v. 4.2.2 (R Core Team, 2022).

3. Results

3.1. Chronology

Magnetostratigraphy Final mean directions, K and paleolatitudes for the various block samples (layers) are presented in SOM Table S2. Sample layer NPO3 and NP04L within the SR-1 paleosol record normal magnetic polarity, with intermediate directions from layer NP04U at the top of the paleosol. The phonolitic tuff (layers NP05-07) records consistent reversed to intermediate reversed polarity directions but with low paleolatitudes ($-53.5°$ to $-69.4°$), whereas the overlying tuffaceous silt (NP08) records reversed polarity with a high paleolatitude ($-81.9°$).
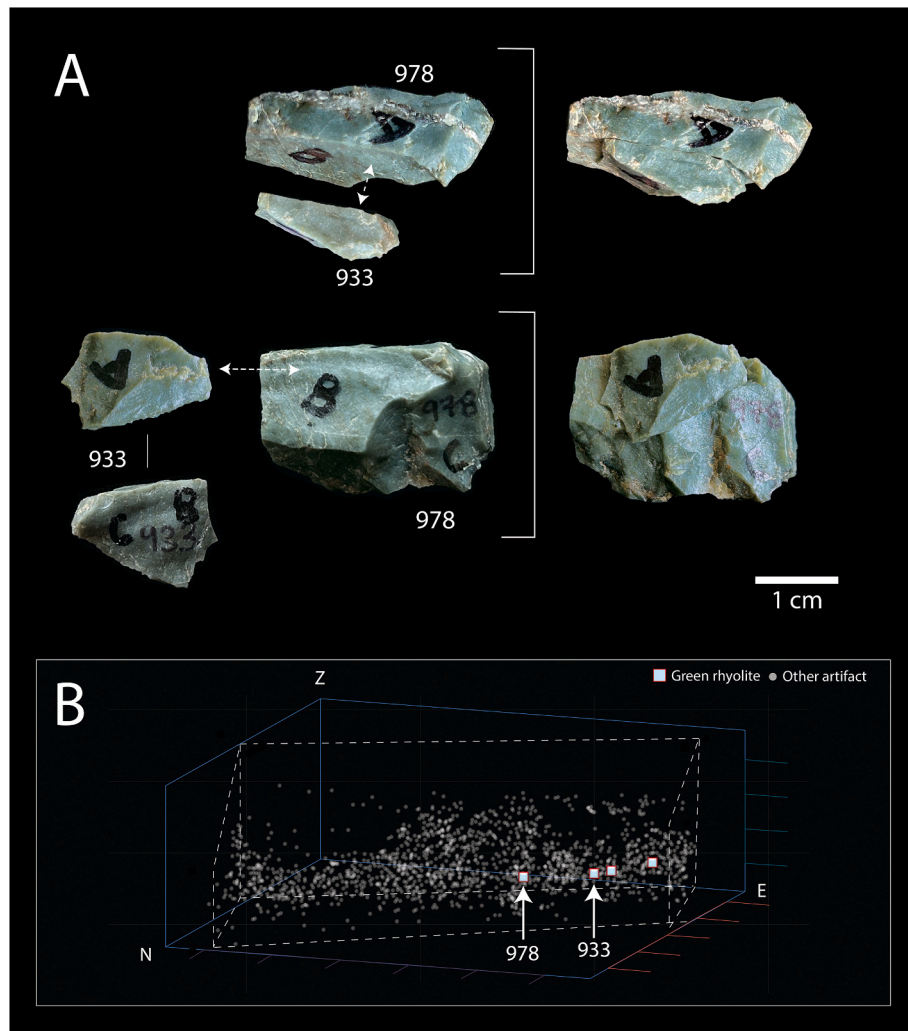
Fig. 12. Lithic refits from excavation 1. A) A fine-grained green rhyolite angular fragment #933 refits with angular fragment #978. B) The location of #978, #933 and other green fine-grained rhyolite lithics (white squares with red outline) are represented relative to the other artifacts in excavation 1. (For interpretation of the references to color in this figure legend, the reader is referred to the Web version of this article.)

Characteristic demagnetization behaviors are evident in Figure 4. Most samples record a single ChRM with some secondary overprinting. Most samples also have highly repeatable sub-sample behavior with high K values even between different demagnetization strategies. However, layer NP07 has highly variable sub-sample behavior and overall steeper inclinations than other samples from the tuff and is therefore defined as intermediate reversed polarity. The normal polarity sample NP03 also has more variable subsample behavior with low K values and a less stable remanence with higher MADs. The samples are stable using AF to between 50 and 80 mT and the remanence in all samples is removed between 500 and 600 °C indicating the remanence is carried by magnetite. High temperature magnetic susceptibility curves also confirm that magnetite is the dominant minerals with Curie Points close to 580 °C (Fig. 5).

Cosmogenic nuclide dating Accelerator mass spectrometry measurements were obtained for both ^{26}Al and ^{10}Be for nine samples taken at Sare-Abururu (SOM Table S3). The sediments sampled are thought to be laterally contemporaneous with those in SR-1 and underlie the tuff which separates SR-1 and SR-2. An average basin altitude of 1259 m was calculated using Shuttle Radar Topography Mission (SRTM) data from the United State Geological Survey (USGS) data server. Assuming that all the samples taken received the same amount of post-burial cosmogenic irradiation, the isochron method (Fig. 6) yields a burial age of 1.512 ± 0.089 Ma (slope $r^2 = 0.97$). All concentrations lie on the same

line, indicating that samples are all consistent with a single age of deposition at the stated time.

3.2. Sedimentology

The Sare-Abururu section is strongly dominated by fine-grained sediments, predominantly silt. They contain a subordinate granule grade component dominated by sub-angular quartz granules largely derived from the underlying heavily weathered granite. Evidence of channelization of flow is rare and channel features are small and shallow (less than 5 m wide and less than 1 m deep). The fill of these channel features is dominated by silts but with an increase in the granule grade component. Cross stratification flow indicators show a large amount of dispersion around a mean flow direction to the southwest towards the Homa Peninsula. These features along with the widespread preservation of the fine-grained tuff layer across the paleolandscape indicate deposition in a low slope, low energy setting.

During SR-2, sediments were primarily deposited via intermittent low energy unconfined fluvial activity resulting in fine-grained sediment throughout. The base of SR-2 is characterized by poorly sorted orange–grey tuffaceous silt with occasional granule grade sediment with infrequent carbonate nodules. This gradationally shifts up the sequence to poorly sorted grey–brown silts with increased carbonate nodule frequency and size.
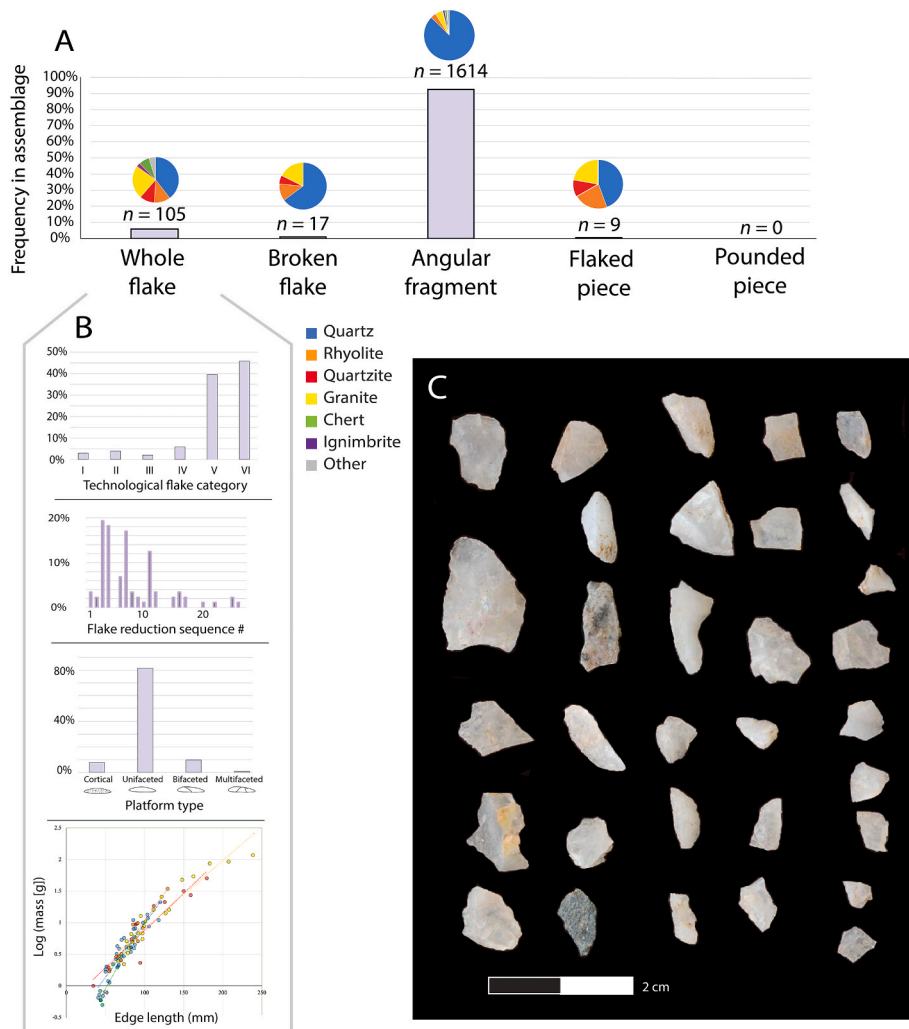
Fig. 13. A) The frequency of tool types in the Sare-Abururu assemblage with the composition of raw materials for tools in each of these categories. B) Flake characteristics, including Technological Flake Category, the reconstructed reduction sequence number calculated with equation #1, platform type and $\log_{10}$ (mass) plotted against edge length (mm) calculated from formula #2, with trendlines grouped by raw material type. C) Photograph of a sample of lithics from Sare-Abururu excavation 1. All pieces are angular shatter with no defined orientation. (For interpretation of the references to color in this figure legend, the reader is referred to the Web version of this article.)

Table 5
Count and percent of raw materials by tool type. Raw materials that constitute more than 1% of the artifact assemblage are included.

Technological category		Quartz		Quartzite		Rhyolite		Granite		Chert		Ignimbrite		Total
		n	%	*n*	%	*n*	%	*n*	%	*n*	%	*n*	%	
FP		4	0.3	1	3.0	2	2.7	2	2.0	0	0	0	0.0	9
DP	Whole flake	41	2.8	12	36.4	12	16.4	25	24.5	8	32.0	3	13.0	105
	Broken flake	11	0.7	1	3.0	1	1.4	3	2.9	0	0.0	0	0.0	17
	Angular fragment	1415	96.2	19	57.6	58	79.5	70	68.6	17	68.0	20	87.0	1614
	Total DP	1467	99.7	32	97.0	71	97.3	0	0.0	0	0.0	0	0.0	1736
PP		0	0.0	0	0.0	0	0.0	0	0.0	0	0.0	0	0.0	0
Manuport		0	0.0	0	0.0	0	0.0	1	1.0	0	0.0	0	0.0	2
Total		1471		33		73		102		25		23		1747

Abbreviations: FP = flaked piece; DP = detached piece; PP = pounded piece.

Excavation 1 at Sare-Abururu is 1.6 m in depth (Fig. 7). Its base is composed of a massive poorly sorted orange–grey tuffaceous silt, with occasional carbonate nodules. Overlying this at 1.1 m in depth is a massive poorly sorted grey–brown silt with frequent carbonate nodules. Occasional roots are also present in the upper part of this horizon. This is overlain by a dark brown–black silty topsoil at 0.4 m in depth.

Excavation 5 is 1.8 m in depth (Fig. 7). At its base is the same massive poorly sorted orange–grey tuffaceous silt as in excavation 1, although

occasional granule grade sediment is present. Carbonate nodules are also present throughout the horizon. This gradationally changes into a massive poorly sorted grey–brown silt at 1.4 m; occasional granules remain present. At 1 m, a gradational change into finer brown silts occurs. Carbonate nodules also increase in presence and size, with some reaching up to pebble size.

Excavation 4 is 1.4 m in depth (Fig. 7). Its base is a poorly sorted grey–brown granular silt. Within this are coarser orange silts. Unlike the

Table 6
The dimensions and characteristics of whole flakes in the Sare-Abururu assemblage. Raw materials that constituted more than 5% of flakes are shown.

		Chert (n = 8)	Granite (n = 25)	Quartzite (n = 12)	Quartz (n = 41)	Rhyolite (n = 12)	Total (n = 105)
Weight (g)	Mean	2.1	23.9	16.4	5.1	8.0	11.6
	Std dev	1.8	31.8	15.3	4.7	9.4	19.3
	Range	0.5–5.1	2.2–117.5	2.0–50.4	0.7–21.1	1.7–34.4	0.5–117.5
Max dimension (mm)	Mean	23.6	44.6	41.4	28.8	31.6	34.6
	Std dev	7.2	17.5	17.3	8.6	9.2	14.7
	Range	17.3–35.6	25.3–97.6	19.7–73.1	15.3–49.7	18.9–49.8	15.3–97.6
Technological length (mm)	Mean	17.6	34.7	32.3	22.8	26.4	27.3
	Std dev	6.3	14.8	14.3	8.5	9.9	12.8
	Range	11.8–27.4	14.1–71.3	14.5–58.2	11.5–45.2	16.0–45.1	11.5–71.3
Maximum width (mm)	Mean	17.9	34.6	33.2	22.1	21.5	26.8
	Std dev	5.9	15.2	12.8	6.7	5.3	12.5
	Range	12.4–30.0	13.4–78.0	14.6–54.8	8.9–36.8	15.2–34.7	8.9–78.0
Technological width (mm)	Mean	16.9	28.4	30.1	19.9	18.5	23.0
	Std dev	5.2	11.4	11.7	6.1	4.5	10.0
	Range	11.8–26.0	13.2–59.3	13.9–46.2	8.8–36.9	13.9–30.1	8.8–60.9
Flake maximum thickness (mm)	Mean	4.9	13.5	11.0	7.9	10.2	9.8
	Std dev	1.8	7.4	4.3	2.9	4.8	5.4
	Range	2.4–7.3	4.4–28.7	3.6–16.7	3.3–15.6	4.3–21.1	2.4–28.7
Flake thickness at 25% (proximal)(mm)	Mean	4.2	11.3	9.7	7.3	8.9	8.6
	Std dev	1.8	6.7	4.0	2.9	3.2	4.6
	Range	2.4–7.3	4.3–27.2	3.4–16.5	3.0–15.6	5.0–16.3	2.4–27.2
Flake thickness at midpoint (mm)	Mean	4.3	11.0	9.1	6.4	8.7	8.0
	Std dev	1.8	6.0	3.7	2.5	4.4	4.4
	Range	2.2–6.3	4.1–27.3	2.8–13.2	2.4–12.1	4.8–19.5	2.2–27.3
Flake thickness at 75% (distal) (mm)	Mean	3.7	9.5	8.0	5.5	7.1	6.9
	Std dev	2.0	5.9	3.4	2.2	4.8	4.2
	Range	1.4–6.4	3.2–25.7	2.2–12.8	1.5–10.2	2.5–18.4	1.4–25.7
Platform depth (mm)	Mean	3.1	9.8	9.1	6.0	5.8	7.1
	Std dev	0.7	6.5	4.1	2.8	2.5	4.4
	Range	2.1–4.1	1.9–23.8	3.5–167.0	2.7–14.4	2.6–10.7	1.9–23.8
Platform length (mm)	Mean	12.2	23.2	23.5	14.8	14.5	17.8
	Std dev	3.	11.7	11.3	4.9	4.7	8.7
	Range	6.1–16.8	8.3–52.4	7.6–52.2	6.6–25.7	7.0–22.3	6.1–52.4
Number of platform facets	Mean	1.5	0.9	1.0	1.0	1.2	1.0
	Std dev	0.5	0.3	0.6	0.4	0.8	0.5
	Range	1–2	0–1	0–2	0–2	0–3	0–3
Number of dorsal scars	Mean	2.1	2.1	2.2	1.6	3.2	2.0
	Std dev	1.2	1.4	1.6	1.1	1.8	1.4
	Range	0–4	0–5	0–6	0–4	1–7	0–7
Width/length	Mean	1.0	0.9	1.0	0.9	0.8	0.9
	Std dev	0.2	0.3	0.4	0.3	0.2	0.3
	Range	0.7–1.4	0.5–1.8	0.6–1.8	0.39–1.51	0.4–1.2	0.4–1.8
Width/thickness	Mean	4.3	3.0	3.5	3.5	2.4	3.3
	Std dev	1.1	1.3	0.7	1.3	0.7	1.2
	Range	2.7–5.7	1.4–6.1	2.8–5.1	1.7–7.7	1.5–3.7	1.4–7.7
Platform depth/platform length	Mean	0.3	0.4	0.4	0.4	0.4	0.4
	Std dev	0.1	0.2	0.1	0.2	0.1	0.2
	Range	0.2–0.4	0.1–0.9	0.2–0.7	0.2–1.2	0.2–0.5	0.1–1.2
Reconstructed edge length (mm)	Mean	59.1	113.0	103.3	74.8	81.7	89.5
	Std dev	17.6	45.3	43.6	20.9	22.6	38.4
	Range	43.3–84.4	66.2–238.6	34.4–179.4	40.7–120.1	55.0–129.6	34.4–238.6
Edge length (cm)/log10 (mass [g])[a]	Mean	14.5	11.7	11.5	13.4	12.0	12.5
	Std dev	2.3	2.9	3.4	4.2	4.3	3.6
	Range	11.9–17.4	8.6–21.6	8.8–18.1	8.2–22.5	8.0–21.7	8.0–22.5
Dorsal cortex (%)	Mean	11%	33%	47%	32%	30%	32%
Feather terminations (%)	Mean	88%	84%	100%	95%	73%	92%
Flakes with cortical platforms (%)	Mean	0%	4%	25%	12%	9%	10%
Platform cortex (%)	Mean	0%	4%	23%	10%	9%	8%

Std dev = standard deviation.
[a] Only flakes over 20 mm in maximum dimension were included in this calculation.

other excavations, carbonates are not present. Some root casts are present. This gradationally shifts into the overlying poorly sorted granular orange silts at 0.6 m. Very infrequent traces of carbonate nodules are present in this horizon. This gradationally shifts into an orange–grey poorly sorted granular silt; only a change in color can be observed.

3.3. Stable isotopic analysis of pedogenic carbonates and paleosol bulk organic matter

The average carbon isotope composition of all paleosol carbonates collected from sediments in the lower unit (SR-1) is −5.7 ± 3.0‰, ranging from −8.9‰ to −2.2‰ (Table 1). The average $\delta^{13}C$ of pedogenic

Fig. 14. Photographs of flakes recovered from excavation 1. Dorsal and ventral surfaces are shown. From left to right (top): quartzite flake #443, quartz flake #1339, quartzite cortical flake #1108. Bottom: granite flake #520, granite flake #1300, quartzite flake #396.

Table 7
Reported flake dimensions from assemblages where the majority of tools were manufactured from quartz (Ludwig, 1999; de la Torre, 2004; de la Torre and Mora, 2018; Braun et al., 2019). Bipolar and freehand experimental assemblages manufactured from Naibor Sor quartzite/quartz are also reported (Byrne et al., 2016).

	n	Age (Ma)	Flake mean length (mm)	Flake mean width (mm)	Flake mean thickness (mm)
HWK EE	1368	1.7	31.0	22.7	11.8
Omo57	44	2.3	24.8	20.4	7.7
Omo123	110	2.3	20.8	17.8	5.9
DK	115	1.8	40.2	37.4	11.9
FLK Zinj	125	1.8	36.8	32.9	26.5
Bipolar	90	experimental	44.0	35.0	13.0
Freehand	108	experimental	42.0	37.0	12.1
Sare (quartz)	41	1.7	22.8	19.9	6.4
Sare (total)	105	1.7	27.3	23.0	8.0

Table 8
Attributes of the Sare-Abururu lithic assemblage compared to the early Oldowan lithic assemblage at Nyayanga. The average cutting edge/mass ratio was calculated as the average edge length (calculated with formula #2, converted into cm) divided by the $\log_{10}$ of mass (g) for each whole flake in the assemblage.

	Sare-Abururu assemblage	Nyayanga assemblage
Percent detached pieces	99.6%	76.4%
Avg. flake cutting edge/mass	12.5 ± 3.6	10.01 ± 2.63
Avg. flake platform depth (mm)	7.1 ± 4.4	9.0 ± 4.9
Avg. flake platform length (mm)	17.8 ± 8.7	20.8 ± 10.2
Avg. artifact density/m³	57.3 artifacts/m³	2.2 artifacts/m³

Avg. = Average.

carbonates from the upper unit (SR-2) is −0.9 ± 1.0‰, with a range from −2.6‰ to 1.0‰ (Table 1). Among carbonates collected in archaeological excavations, the average δ^{13}C is −1.0 ± 0.0‰, −1.3 ± 0.7‰ and −0.5 ± 1.1‰ for excavations 1, 2 and 5, respectively (Table 1).

Among samples in the top 15 cm of the paleosol horizon, the average carbon isotopic composition of paleosol bulk organic matter is −14 ± 0.8‰, and the average carbon contents (%C) of the bulk organic matter samples is 0.1%, ranging from 0.1% to 0.2% (Table 2). There is no significant correlation ($p > 0.05$) between δ^{13}C and %C, which indicates that carbon isotopic variation in paleosol bulk organic matter likely reflects variation in original plant biomass rather than decomposition or modern contamination. To further address the use of bulk organic matter δ^{13}C for reconstructing paleovegetation, additional samples were collected at increasing depth from the paleosol horizon surface below two samples in the top 15 cm (SR14-1 and SR14-7) (Table 2). In the SR14-1 depth profile we find a relatively consistent carbon isotopic composition (−12.8 ± 0.4‰). In the SR14-7 depth profile we find lower δ^{13}C (−15.4 ± 0.8‰) closer to the surface (≤45 cm) and higher δ^{13}C (−12.6 ± 0.2‰) at greater depths, consistent with effects of decomposition processes (Wynn, 2007).

The carbon isotopic composition of pedogenic carbonates and paleosol organic matter from SR-1 and SR-2 indicates that grasslands (<10% woody cover) were likely prevalent, possibly also including open woody grasslands (~10–20% woody cover; Fig. 8A). A small number ($n = 3$) of pedogenic carbonates from SR-1 indicates the presence of more wooded vegetation typical of a grassy woodland/bushland/shrubland (~40–60% woody cover).

Excavated lithics at Sare-Abururu were deposited within a grassland environment similar to the context of the Oldowan locality of Kanjera South (Fig. 8). This contrasts with a number of other Early Stone Age lithic sites across eastern Africa where the carbon isotopic compositions of associated pedogenic carbonates indicate local vegetation dominated by wooded grasslands (~20–40% woody cover) to open woodland/bushland/shrublands (~40–60%).

3.4. Lithic assemblage

In total, 1745 in situ lithics were recovered. Artifacts were found in all five excavations, but their density varied considerably by site.
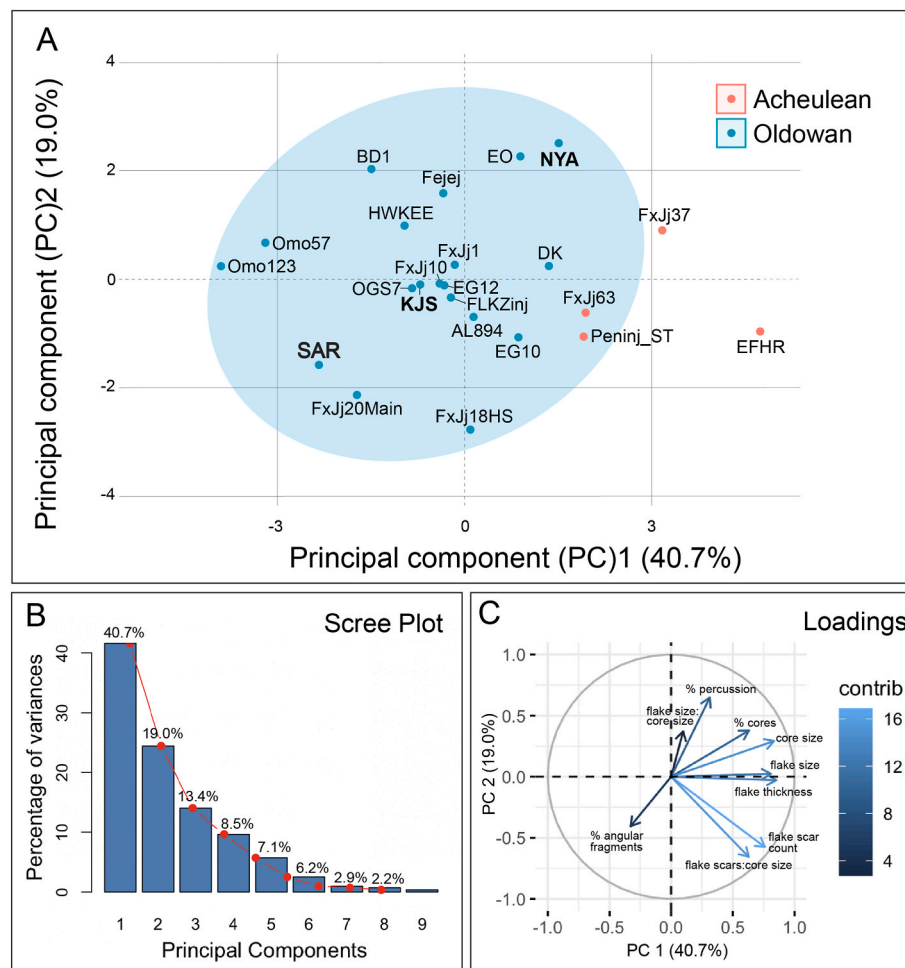
Fig. 15. Principal component analysis based on major technological attributes of Early Stone Age artifact assemblages (SOM Tables S4–S7). A) Assemblages are plotted according to principal component (PC) 1 (x-axis) and PC 2 (y-axis). The Sare-Abururu assemblage (SAR) falls within the shaded ellipse that represents the 95% confidence interval for Oldowan sites. B) A scree plot with eigenvalue percentage of variance for PCs 1–9. C) Loadings are plotted for PC 1 and PC 2 with the contribution of each variable are shown below.

Excavation 1 (Fig. 9) preserved a denser accumulation (*n* = 1651; 86 artifacts/m³) than excavation 2 (*n* = 10; 3 artifacts/m³), excavation 3 (*n* = 4; 2 artifacts/m³), excavation 4 (*n* = 56; 20 artifacts/m³) and excavation 5 (*n* = 24; 7 artifacts/m³). Although the samples from excavations 2–5 are not robust enough to draw meaningful comparisons between excavations, in each trench quartz is the most common raw material and the maximum dimension of lithics is small. There is a high frequency of debitage measuring under 20 mm (*n* = 682, 39.1% of the assemblage).

Small vein quartz pebbles are locally available in a paleochannel conglomerate in the amphitheater within 100–300 m of all excavations (Fig. 10; see also Fig. 3B). Out of the 500 cobbles randomly sampled from this conglomerate, the most common raw material is quartz (46%), followed by rhyolite (41%), quartzite (7%) and granite (3%). The size of available clasts is small, with most measuring under 25 mm in maximum dimension (58%), and nearly all available materials measuring under 45 mm (96%). The abundance of quartz pebbles in the local paleo-drainage is reflected in the lithic assemblage. Sare-Abururu artifacts were made from 84.3% quartz (*n* = 1471). A variety of other raw materials are present in small proportions in the assemblage including granite (*n* = 102), quartzite (*n* = 33), rhyolite (*n* = 73), chert (*n* = 25) and ignimbrite (*n* = 23).

Artifact raw materials do not directly reflect local availability, indicating that hominins were still selective in the materials they used to produce tools. When the Sare-Abururu assemblage is compared to expected lithologies based on the paleo-drainage raw material frequency, there are significant differences between the artifact and conglomerate samples (X^2 = 813.3, *n* = 3409, df = 4, *p* < 0.001; Table 3). Quartz, chert and granite were selected more frequently than expected, while quartzite and rhyolite were selected less frequently than expected based on availability (Table 3).

The distribution of lithic raw materials varied spatially across sites and within excavations. Stone tools recovered from excavation 1 (*n* = 1641) were manufactured predominantly from quartz (85.1%). Quartz is also the most common material in excavations 2–5 (72.2%). However, rhyolite, chert and quartzite raw materials are present in slightly higher proportions relative to excavation 1 (Table 4). Granite, the second most frequent raw material in excavation 1 (*n* = 102; 6.1%), is an exception; only two granite artifacts were recovered from excavations 2–5.

Although artifact accumulations were dense throughout excavation 1, lithic raw materials were not uniformly distributed. For example, all 28 quartzite lithics recovered from excavation 1 were concentrated towards the east side of the excavations and absent from the four squares nearest to the west (Fig. 11). Four pieces of fine-grained green rhyolite were recovered from neighboring squares at similar elevations (Fig. 12). Two of these pieces (#933 and #978) refit (Fig. 12). Both are angular fragments; #933 is an angular fragment with a crushed platform and artifact #978 preserves the scars from two flakes that were removed after #933 was detached. These two artifacts were found within the
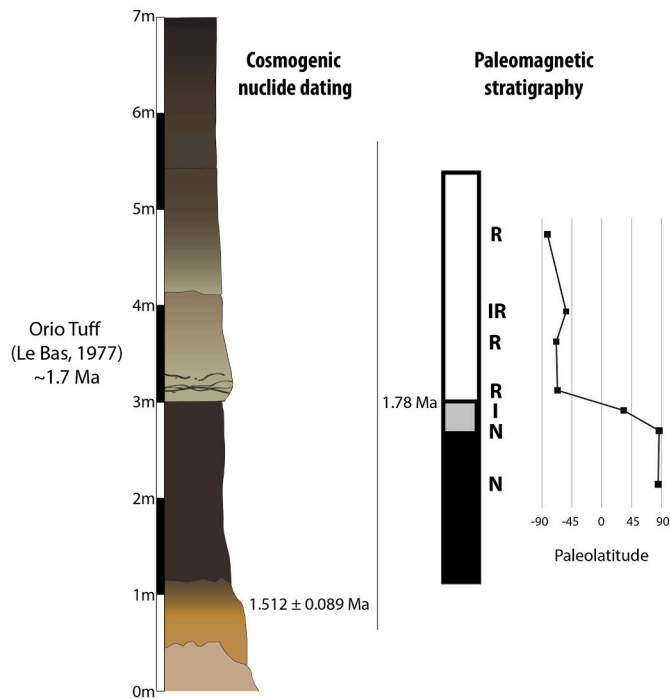
Fig. 16. Sare-Abururu composite stratigraphic section with chronological framework. The 1.7 Ma phonolitic tuff date derives from the whole rock K/Ar date of the Nyamatoto plug, the likely source of the tuff (Le Bas, 1977). Paleomagnetic stratigraphy and cosmogenic results are from the current project.
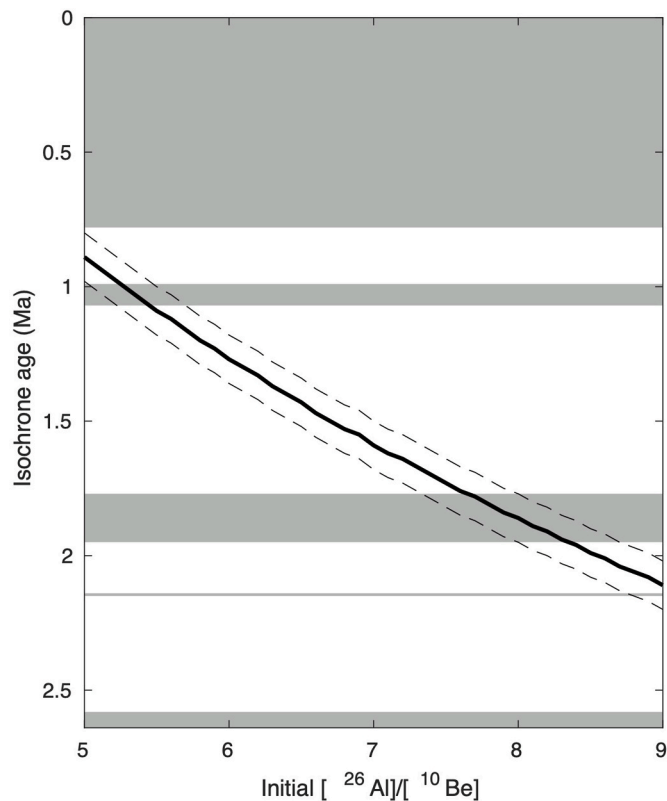

Fig. 17. The relationship between isochrone age and initial production rate ratio. Isochrone age (y-axis) estimates change with the ^{26}Al/^{10}Be production ratio (x-axis). Shaded areas denote periods of normal polarity.

same spit and at the same approximate elevation. Artifact #978 was recovered 0.9 cm above #933 and approximately 89 cm apart on the north and east axis.

The Sare-Abururu assemblage is almost entirely composed of angular shatter (92.5%; Fig. 13). A modest number of whole flakes and broken flakes are also preserved (7.0%). However, cores are nearly absent; only nine were recovered, representing 0.5% of the assemblage. Angular shatter disproportionately derived from quartz pieces (87.7%), while flakes and cores are more representative of other lithologies, such as granite, rhyolite and quartzite (Fig. 13; Table 5).

Because of the small sample size, few conclusions can be drawn from the flaked pieces category. However, it is worth noting that the maximum dimensions of cores (mean = 47.9 mm ± 17.8) place them among the largest of locally available pebbles. There is also a great deal of variability in the degree of reduction. The percentage of remnant cortex ranges from 0 to 80% (mean = 30.7% ± 31.9) and the number of flake scars ranges from 1 to 8 (mean = 5.2 ± 3.5). The length (mean = 29.0 mm ± 19.8) and width (mean = 24.0 mm ± 12.6) of the longest flake scars on each core removal surface are within the range of whole flakes in the assemblage (Table 6). Cores are unifacial (*n* = 2), bifacial (*n* = 3) and multifacial (*n* = 4). A single invasive flake was removed from one granite and one rhyolite unifacial core. Two bifacial cores were exploited by unidirectionally flaking two adjacent surfaces of a rounded quartz cobble and an angular rhyolite clast. Another bifacial core made from quartzite was worked centripetally. The multifacial cores were reduced irregularly on quartz (*n* = 3) and granite (*n* = 1) until little remnant cortex remained (mean cortex = 5% ± 5.8). The maximum dimensions of multifacial cores (mean = 41.0 mm ± 18.9) are on average less than bifacial (mean = 47.4 mm ± 14.7) and unifacial (mean = 62.5 mm ± 20.5) cores. Because only nine cores were recovered, the implication of these observations is uncertain.

Whole flakes make up a more substantial part of the assemblage (*n* = 105) and are therefore more informative. Most flakes end in feather terminations and possess a single bulb and platform (Fig. 14). Flakes were assigned to Technological Flake Categories based on the amount of cortex on the platform and dorsal surface (Fig. 13). The Type VI category contains the highest number of flakes (45.6%) followed by Type V (39.8%). Early-stage flakes are present in small proportions, including Type I (2.9%), showing that early-stage reduction also occurred to some extent at Sare-Abururu. Type II (3.9%) and Type III (1.9%) flakes are also represented. Flake reduction sequence number was estimated using a multiple linear regression of the flake stage that accounts for initial core size (Braun et al., 2008b; formula 1). The results indicate that the assemblage contains flakes from both the beginning and end of reduction sequence (Fig. 13). Most flakes occur within the first 10 removals, consistent with the early-stage reduction of raw materials from local sources.

Platform depth is low (mean = 7.1 mm ± 4.2) relative to platform length (mean = 17.8 mm ± 8.7) and over 10% of platforms are bifaceted or multifaceted (Fig. 13). Two detached pieces were retouched around the edge, both of which were manufactured from rhyolite. A high proportion of flakes end in feather terminations (91.7%), despite the fracture unpredictability of quartz. Only 13.3% of quartz flakes with dorsal scars (*n* = 30) possess accidental scars. Of the dorsal scars on quartz flakes (*n* = 44), 9.1% are hinge or step scars. These values are relatively low compared to the frequency of accidental flake scars reported elsewhere (Hovers, 2009).

Flake dimensions show affinities to the flake assemblage at Omo123 with respect to technological length, width and thickness (Table 7). At Omo123 and Sare-Abururu, flakes are small in size and the relationship between technological length, width and thickness is similar. The relationship between cutting edge and mass is consistent across raw material types, including quartz (Fig. 13; Table 6). The ratio of cutting edge to mass is within the range of published values from Kanjera South (Reeves et al., 2021). Sare-Abururu flakes over 20 mm in maximum dimension (*n* = 82) yield a mean edge to mass ratio of 12.5. Quartz flakes (*n* = 29)

have slightly higher ratios (13.4) and are similar to the values reported for the raw material with the highest cutting edge to mass ratios at Kanjera South (Nyanzian rhyolite, Reeves et al., 2021).

In contrast to Nyayanga, the Sare-Abururu assemblage consists almost exclusively of detached pieces with a very low frequency of flaked pieces and an absence of tools with evidence of percussive activities. At the Sare-Abururu locality, artifact accumulations are also denser than at Nyayanga (Table 8). A PCA was carried out based on technological attributes of artifact assemblages from the Early Stone Age (Fig. 15; SOM Tables S4–S6). We considered the scores for principal component (PC) 1 (40.7%) and PC 2 (19.0%) because they represent most of the variation between assemblages. The variables that load most heavily on PC1 are the average flake maximum dimension and thickness, average core size and average number of flake scars. The variables that load most heavily on PC 2 are the ratio of flake scars to core size, percussion frequency, the number of flake scars and the frequency of angular fragments. The Sare-Abururu, Kanjera South and Nyayanga assemblages fall within the 95% confidence interval of Oldowan sites based on PC 1 and PC 2. However, the Homa Peninsula sites exhibit substantial variation within the broader Oldowan sample. The assemblage most similar to Sare-Abururu on PC1 and PC2 is FxJj 20 Main. The Sare-Abururu assemblage is distinct from the Acheulean sample mean (EFHR, FxJj63, Peninj and FxJj37) (Fig. 15).

4. Discussion

4.1. Age of hominin activity

All lines of chronological evidence point to an age younger than Kanjera South (Fig. 16). Deposition was expected to occur ca. 1.7 Ma based on the whole rock K/Ar date of 1.73 ± 0.06 Ma of the Nyamatoto plug, the likely source of the phonolitic tuff (Le Bas, 1977), which is bracketed by SR-1 and SR-2. Magnetostratigraphy is consistent with this expectation. The normal polarities underlying intermediate polarity in SR-1 are overlain by consistent reversed polarity in the phonolitic tuff and throughout SR-2. We interpret the change from normal, through intermediate and into reversed polarity, as the reversal at the end of the Olduvai subchron at ~1.775 Ma (Ogg, 2020). This means that the phonolitic tuff and Oldowan stone tools in SR-2 are within the C1r.3r subchron of the Matuyama Chron younger than ~1.775 Ma, and the SR-1 paleosol was deposited prior to this, within the Olduvai subchron (~1.95–1.78 Ma). The intermediate polarity at the top of the SR-1 paleosol and the overall low paleolatitude values in the reversed polarity phonolitic tuff suggest these sediments were deposited during and very soon after the upper Olduvai reversal at 1.775 Ma, with the field yet to fully stabilize. This is consistent with and within the error of a tuff age of 1.73 ± 0.06 Ma. The uppermost deposit in SR-2 records stable reversed polarity and high paleolatitude values that are consistent with the deposits and archaeology being deposited once the field has stabilized after the upper Olduvai reversal at 1.775 Ma.

Cosmogenic dates yield an age estimate of 1.512 ± 0.089 Ma for samples collected from the base of SR-1, younger than estimates provided by the other chronological dating methods. While it is possible that the two normal and intermediate polarity recorded within SR-1 represents the Gilsa event at 1.567–1.575 Ma (Singer, 2014), which is within the error range of the cosmogenic age estimate, the recording of a short magnetic event within such a sequence is much less likely. It is standard to assume an initial production rate of 6.75 26Al/10Be, but this estimation is known to be imprecise and to vary with altitude, latitude and depth (Fenton et al., 2022). For example, empirical 26Al/10Be concentrations can reach up to 8 at 1–2 m under the surface (Balco, 2017; Rodés, 2021). A higher production rate ratio of 7.8 ± 0.3 would produce an age of 1.78 Ma (Fig. 17). This is a more likely local production rate ratio for the Sare-Abururu locality based on the paleomagnetic evidence, and similar surface production rate values have been

suggested for other sites (e.g., Goethals et al., 2009). This improved local production rate will help future studies using burial dating in the Sare-Abururu region.

Taken together, evidence from multiple dating methods is most consistent with an interpretation that the Sare-Abururu upper paleosol and associated artifacts were deposited <1.78 Ma. This interpretation is also in agreement with the expected regional depositional sequence of Homa Peninsula sediments developed by Le Bas (1977) with the Sare-Abururu sequence occurring between the deposition of the Kanjera South Member of the Kanjera Formation ending around 1.95 Ma, and the base of the Kanjera North Member at less than 1.5 Ma (Bishop et al., 2022).

4.2. Oldowan activity at Sare-Abururu

Analysis of paleosol carbonates indicates that Sare-Abururu hominins manufactured tools in a grassland dominated ecosystem similar to Kanjera South. Tool accumulations were spatially concentrated at excavation 1, where most lithics were recovered. Sediment analysis from excavation 1 indicates low-energy, relatively undisturbed silts and muds. The characterization of sediments in excavation 1, coupled with the quantities of recovered lithics, and the presence of a technological refit, indicate that numerous undisturbed in situ knapping events occurred here. The abundance of debris measuring under 20 mm is suggestive of on-site flaking. The distribution of Technological Flake Categories closely resembles the complete flake profiles produced from experimental replications of assemblages with strong bifacial and multifacial components (Toth, 1987). Sare-Abururu flake types are similar to experimental replications of FxJj 10 (Toth, 1987), an assemblage where the majority of cores were exploited using bifacial or multifacial reduction. However, the relatively low frequency of whole flakes and the near absence of cores at Sare-Abururu suggest that some tools, especially cores that still had utility, were likely transported away from the knapping site and discarded elsewhere.

Despite the favorable depositional environment for lithics, fossilized bone remains are not preserved in any excavations, probably because of the proximity of the archaeological levels to the granite bedrock, which lowered groundwater pH during the deposition of the sediments. Although it appears that the technology focused on the production of flakes for cutting behaviors, whether these flakes were used for butchery is unknown. Macroscopic use-related damage is present on some artifacts, suggesting that future use-wear analyses as carried out on Kanjera South and Nyayanga artifacts (Lemorini et al., 2014, 2019; Plummer et al., 2023) may help define the function of Sare-Abururu tools.

Determining the flake production strategy employed by Sare-Abururu hominins is made difficult by the fragmentary nature of the assemblage. Elsewhere, quartz shatter is often associated with bipolar techniques (Gurtov and Eren, 2014), although free-hand percussion is also common (de la Torre, 2004). However, at Sare-Abururu, the absence of cores, hammerstones, anvils, or diagnostic features on the majority of quartz lithics makes it difficult to draw conclusions about the specific flaking technique. The presence of bifaceted and multifaceted platforms on whole flakes supports some degree of direct freehand percussion. Flake proportions, including length, width and thickness, are similar to experimental assemblages produced by freehand percussion (Byrne et al., 2016; Fig. 15). Other features of flakes, including the high frequency of feather terminations and the ability to maximize cutting edge while minimizing mass, suggest that toolmakers did not lack refined flaking abilities. It is possible that the Sare-Abururu assemblage was formed by a combination of techniques, including freehand reduction, and that quartz pebbles could have been reduced differently than other lithologies.

4.3. Oldowan behavioral variability

Sare-Abururu, Kanjera South and Nyayanga span nearly the entire

duration of the Oldowan Industrial Complex, allowing us to consider how stone tool activities vary regionally on the peninsula and through evolutionary time. On the Homa Peninsula, a range of Oldowan technological behaviors occurred within an open grassland context during the Early Pleistocene, which stands in contrast to other Oldowan localities associated with greater amounts of woody cover (Quinn et al., 2013). A variety of Oldowan localities elsewhere in eastern Africa, including at Nyayanga (Plummer et al., 2023), are situated in open woodland/bushland/shrublands and wooded grasslands (Rogers et al., 1994; Sikes, 1994; Isaac and Behrensmeyer, 1997; Levin et al., 2011). Tree cover may have provided protection for predator avoidance (Blumenschine and Peters, 1998) and shade for thermal stress (Wheeler, 1994). These factors are difficult to assess at Sare-Abururu, especially given the lack of faunal preservation. However, we note that 1) the acquisition and processing of bovids at Kanjera South suggests tree cover was not necessary for predator avoidance (Ferraro et al., 2013; Oliver et al., 2019) and 2) oxygen isotopic analysis of fossil mammal teeth from Kanjera South indicates that low aridity and thus lower thermoregulatory stress may play a role in the use of grasslands by Oldowan hominins (Blumenthal et al., 2017). It is possible that on the Homa Peninsula thermoregulatory constraints were reduced and the activities of Early Pleistocene toolmakers were not limited to areas with more substantial woody cover while making and using tools. The Homa Peninsula data are consistent with temporal trends in the Oldowan record documenting greater artifact concentrations in more diverse environmental settings that include grassland-dominated habitats in assemblages younger than ca. 2 Ma (Rogers et al., 1994; Plummer and Finestone, 2018). The use of grasslands by Oldowan hominins on the Homa Peninsula could relate to a general increase in the representation of C_4 biomass in eastern Africa through the Early Pleistocene (Uno et al., 2016), the local abundance of C_4 vegetation, or potentially to a local preference for grasslands or other correlated biotic or abiotic factors.

In addition to paleohabitat, the distribution of stone raw material sources is known to drive variation in raw material use and reduction (Andrefsky, 1994, 2009; Dibble, 1995; Kuhn, 2004; Dibble et al., 2017; Reeves et al., 2021). Sare-Abururu hominins used local stone materials and employed simple reduction strategies. Toolmakers almost exclusively selected quartz pebbles and generally avoided other hard and durable lithologies, such as rhyolite and quartzite, that are known to fracture more predictably than quartz (Braun et al., 2009a). The result is a Sare-Abururu assemblage dominated by angular shatter, likely a byproduct of the mechanical properties of vein quartz (Tallavaara et al., 2010; Driscoll, 2011). This deviates from the strategies of Kanjera South hominins who used quartz but prioritized more easily flaked quartzite and rhyolite (Braun et al., 2008a) and reduced cores in more systematic and technologically complex sequences. This difference can be partly explained because lithic accumulations at Sare-Abururu were formed very close to abundant naturally occurring durable materials, whereas local lithologies were relatively soft at Kanjera South, perhaps providing the impetus for the strategic economization of harder raw materials. Although rhyolite and quartzite clasts were locally available to Sare-Abururu, hominins selected these raw materials less frequently than expected based on their availability.

In contrast to the Oldowan technological strategies at Nyayanga (Plummer et al., 2023), Sare-Abururu toolmakers produced hundreds of detached pieces with cutting edges with little to no emphasis on pounding/percussive tools in the assemblage. It is possible that the narrow band of woodland resources along the stream exploited by Nyayanga hominins required a greater degree of processing by pounding than foods abundant in the grassland dominated habitats of other Homa Peninsula localities. Although the total number of artifacts recovered at Sare-Abururu was larger, the emphasis on small angular fragments, as opposed to larger flakes, cores and pounding tools, impacts this comparison. The overall weight of lithic material recovered at Nyayanga and Sare-Abururu was comparable and artifact density at Sare-Abururu

varied substantially across the landscape. Artifact scatters were concentrated at excavation 1, but sparse in the other excavations. Sare-Abururu toolmakers maximized flake cutting edge and controlled platform depth more consistently than the earliest toolmakers known from the Homa Peninsula at Nyayanga (Table 8).

It appears that stone tool production at Nyayanga, Kanjera South and Sare-Abururu differed with respect to raw material utilization and assemblage composition but was well suited in each case to the context of their local landscapes and ecology. The paleoenvironmental contexts at Nyayanga, Kanjera South and Sare-Abururu each contained different features that could have attracted hominins and shaped tool-assisted foraging in diverse ways. At Nyayanga, fresh water, access to a variety of plant and animal tissue and perhaps proximity to tree cover, provided an attractive setting for these Late Pliocene hominins. These hominins relied on both cutting and pounding tools to access locally available meat, marrow and plant materials (Plummer et al., 2023). Around 2 Ma, Kanjera South lacked the refuge of a more wooded habitat and high-quality stones were not available in the local stream channel, but food resources were likely abundant; persistent access to meat, marrow and plant foods likely attracted hominins to repeatedly return to this location with exotic durable stone materials (Braun et al., 2009b; Ferraro et al., 2013; Lemorini et al., 2014). On the eastern margin of the Homa Peninsula, Sare-Abururu hominins manufactured small cutting tools near naturally occurring sources of small quartz pebbles. The local abundance of durable quartz stone and accessibility to open grassland resources may have attracted hominins forming the Sare-Abururu assemblage around 1.7 Ma.

Evidence from the behavioral strategies preserved at Sare-Abururu suggests that the reduction of small quartz pebbles was a reoccurring behavior in the Early Stone Age and was not simply the byproduct of limited knapping ability or raw material access. Similar patterns of quartz shatter have been reported throughout the Oldowan Industrial Complex. Some of the earliest Oldowan toolmakers (2.34 Ma) worked small quartz pebbles in the Shungura Formation in the lower Omo River Valley, Ethiopia (Chavaillon, 1976; de la Torre, 2004; Delagnes et al., 2011). In the Omo-Turkana basin, the Fejej sites (ca. 1.96 Ma) also preserve assemblages produced from quartz pebbles (Barsky et al., 2011; de Lumley et al., 2023), and at Olduvai Gorge, Tanzania, one of the most frequently accessed raw material is CQRM (Crystalline Quartz-rich Raw Material). Though often published as 'quartzite', this material is similar in appearance and in fracture mechanics to quartz (Tarriño et al., 2023). Crystalline Quartz-rich Raw Material was often the preferred raw material in Bed I and became increasingly more dominant through Bed II (Leakey, 1971; Kimura, 2002; de la Torre and Mora, 2005; Diez-Martín et al., 2021, 2022), with the highest proportions known from site BK (Diez-Martín et al., 2009). At sites in the lower Omo River Valley, Fejej and Olduvai, hominins also had access to other materials, but preferentially selected quartz (Diez-Martín et al., 2009; Delagnes et al., 2011), suggesting that the reduction of quartz pebbles was a technical strategy rather than a raw material constraint. Quartz is often difficult to flake, but produces detached pieces with sharp, durable edges, that may have facilitated cutting activities associated with higher edge attrition (Braun et al., 2008b, 2009a). Quartz was also occasionally worked on the Homa Peninsula at Kanjera South (~2% of assemblage). However, other durable materials (e.g., rhyolite and quartzite) were selected more frequently (Braun et al., 2008a).

When compared to other quartz-dominated Oldowan assemblages, Sare-Abururu flakes most closely resemble Omo123 with respect to size and shape (Table 7). These dimensions are similar to assemblages experimentally produced by freehand percussion. Flakes manufactured using freehand techniques tend to be relatively wider and thinner than those made using bipolar percussion (Diez-Martín et al., 2011; Byrne et al., 2016). Overall, the technology at Sare-Abururu showed the most affinity to FxJj 20 Main, an assemblage consisting primarily of basalt (Hlubik et al. 2019). This could be explained by a combination of

technological strategies and similar site formation processes. Like Sare-Abururu, FxJj 20 Main artifacts were preserved in low energy fine silts in a relatively stable depositional environment (Hlubik et al. 2019). The percent of angular fragments are among the highest reported in the Oldowan and relatively few cores were recovered (SOM Table S4).

5. Conclusions

At Sare Abururu, hominins manufactured artifacts ca. 1.7 Ma in a grassland-dominated ecosystem. Artifacts were deposited on an alluvial plain and buried via low energy water flow. In excavation 1, 1641 stone tools were recovered from relatively undisturbed fine-grained silts. Artifacts consisted primarily of quartz angular fragments. Although a range of durable stone materials was locally abundant, hominins at Sare-Abururu opted primarily for small quartz pebbles and underutilized materials that flake more predictably, like rhyolite and quartzite. Quartz is among the most challenging materials to flake; however, Sare-Abururu toolmakers were skilled knappers capable of controlling platform structure and effectively converting mass into cutting edge.

The exploitation of quartz pebbles is a re-occurring strategy throughout the Oldowan Industrial Complex across multiple regions. However, manufacturing small cutting tools from local clasts substantially deviates from toolmaker strategies observed at other sites on the Homa Peninsula. The occurrence of this technological strategy in the same geographic region and in a similar landscape to Kanjera South, where past hominins invested more substantively in lithic transport and reduction, is intriguing. On the Homa Peninsula, tool-assisted dietary flexibility played out in different ways across relatively open habitats, resulting in diverse archaeological assemblages that have the potential to inform on Oldown behavior more broadly.

The number of documented Oldowan sites is limited and localities are rare across Africa. Sare-Abururu expands the regional record in southwestern Kenya and demonstrates a range of technological strategies on the Homa Peninsula wide enough to span much of the variation observed across the entire Oldowan record. The diversity of lithologies and resources available on the peninsula led to substantial heterogeneity in local tool technology. Evidence from Sare-Abururu suggests that Oldowan behaviors were highly flexible and differences between assemblages may reflect variation in local strategies rather than long-term trends in the abilities of toolmakers through time.

CRediT authorship contribution statement

Acknowledgments

Supplementary Online Material

Supplementary Online Material to this article can be found online at https://doi.org/10.1016/j.jhevol.2024.103498.

References

Andrefsky, W., 1994. Raw-material availability and the organization of technology. Am. Antiq. 59, 21–34.

Andrefsky, W., 1998. Lithics: Macroscopic Approaches to Analysis. Cambridge University Press, New York.

Andrefsky, W., 2009. The analysis of stone tool procurement, production, and maintenance. J. Archaeol. Res. 17, 65–103.

Antón, S.C., Leonard, W.R., Robertson, M.L., 2002. An ecomorphological model of the initial hominid dispersal from Africa. J. Hum. Evol. 43, 773–785.

Antón, S.C., Potts, R., Aiello, L.C., 2014. Evolution of early *Homo*: An integrated biological perspective. Science 345, 1236828.

Aronson, J.L., Hailemichael, M., Savin, S.M., 2008. Hominid environments at Hadar from paleosol studies in a framework of Ethiopian climate change. J. Hum. Evol. 55, 532–550.

Balco, G., 2017. Production rate calculations for cosmic-ray-muon-produced 10Be and 26Al benchmarked against geological calibration data. Quat. Geochronol. 39, 150–173.

Balco, G., Rovey, C.W., 2008. An isochron method for cosmogenic-nuclide dating of buried soils and sediments. Am. J. Sci. 308, 1083–1114.

Barsky, D., Chapon-Sao, C., Bahain, J.J., Beyene, Y., Cauche, D., Celiberti, V., Desclaux, E., de Lumley, H., de Lumley, M.A., Marchal, F., Moullé, P.E., 2011. The early Oldowan stone-tool assemblage from Fejej FJ-1a, Ethiopia. J. Afr. Archaeol. 9, 207–224.

Behrensmeyer, A.K., Potts, R., Plummer, T., Tauxe, L., Opdyke, N., Jorstad, T., 1995. The Pleistocene locality of Kanjera, western Kenya: Stratigraphy, chronology and paleoenvironments. J. Hum. Evol. 29, 247–274.

Beuselinck, L., Govers, G., Poesen, J., Degraer, G., Froyen, L., 1998. Grain-size analysis by laser diffractometry: Comparison with the sieve-pipette method. Catena 32, 193–208.

Bishop, L.C., Plummer, T.W., Braun, D.R., Ditchfield, P.W., Goble Early, E., Hertel, F., Lemorini, C., Oliver, J.S., Potts, R., Vincent, T., Whitfield, E., Kinyanjui, R., 2022. Fauna and paleoenvironments of the Homa Peninsula, western Kenya. In: Reynolds, S.C., Bobe, R. (Eds.), African Palaeoecology and Human Origins. Cambridge University Press, Cambridge, pp. 360–375.

Blumenschine, R.J., Peters, C.R., 1998. Archaeological predictions for hominid land use in the paleo-Olduvai Basin, Tanzania, during lowermost Bed II times. J. Hum. Evol. 34, 565–608.

Blumenthal, S.A., Levin, N.E., Brown, F.H., Brugal, J.P., Chritz, K.L., Harris, J.M., Jehle, G.E., Cerling, T.E., 2017. Aridity and hominin environments. Proc. Natl. Acad. Sci. USA 114, 7331–7336.

Braun, D.R., 2005. Examining flake production strategies: Examples from the Middle Paleolithic of southwest Asia. Lithic Technol. 30, 107–125.

Braun, D.R., Harris, J.W., 2003. Technological developments in the Oldowan of Koobi Fora: Innovative techniques of artifact analysis. In: Moreno, J., Torcal, R., Saniz, I. (Eds.), Oldowan: Rather More than Smashing Stones. University of Barcelona Press, Barcelona, pp. 117–144.

Braun, D.R., Plummer, T., Ditchfield, P., Ferraro, J.V., Maina, D., Bishop, L.C., Potts, R., 2008a. Oldowan behavior and raw material transport: Perspectives from the Kanjera Formation. J. Archaeol. Sci. 35, 2329–2345.

Braun, D.R., Pobiner, B.L., Thompson, J.C., 2008b. An experimental investigation of cut mark production and stone tool attrition. J. Archaeol. Sci. 35, 1216–1223.

Braun, D.R., Rogers, M.J., Harris, J.W.K., Walker, S.J., 2008c. Landscape-scale variation in hominin tool use: Evidence from the developed Oldowan. J. Hum. Evol. 55, 1053–1063.

Braun, D.R., Tactikos, J.C., Ferraro, J.V., Arnow, S.L., Harris, J.W., 2008d. Oldowan reduction sequences: Methodological considerations. J. Archaeol. Sci. 35, 2153–2163.

Braun, D.R., Plummer, T., Ferraro, J.V., Ditchfield, P., Bishop, L.C., 2009a. Raw material quality and Oldowan hominin toolstone preferences: Evidence from Kanjera South, Kenya. J. Archaeol. Sci. 36, 1605–1614.

Braun, D.R., Plummer, T.W., Ditchfield, P.W., Bishop, L.C., Ferraro, J.V., 2009b. Oldowan technology and raw material variability at Kanjera South. In: Hovers, E., Braun, D.R. (Eds.), Interdisciplinary Approaches to the Oldowan. Springer, Dordrecht, pp. 99–110.

Braun, D.R., Harris, J.W., Levin, N.E., McCoy, J.T., Herries, A.I., Bamford, M.K., Bishop, L.C., Richmond, B.G., Kibunjia, M., 2010. Early hominin diet included diverse terrestrial and aquatic animals 1.95 Ma in East Turkana, Kenya. Proc. Natl. Acad. Sci. USA 107, 10002–10007.

Braun, D.R., Plummer, T.W., 2013. Oldowan technology at Kanjera South: Technological diversity on the homa peninsula. In: Sahnouni, M. (Ed.), Proceedings of the International Symposium "Africa: Cradle of Humanity: Recent Discoveries." Travaux du Centre National de Recherches Prehisoriques, Anthropologiques et Historiques, vol. 18, pp. 131–145.

Braun, D.R., Aldeias, V., Archer, W., Arrowsmith, J.R., Baraki, N., Campisano, C.J., Deino, A.L., DiMaggio, E.N., Dupont-Nivet, G., Engda, B., 2019. Earliest known Oldowan artifacts at >2.58 Ma from Ledi-Geraru, Ethiopia, highlight early technological diversity. Proc. Natl. Acad. Sci. USA 116, 11712–11717.

Byrne, F., Proffitt, T., Arroyo, A., de la Torre, I., 2016. A comparative analysis of bipolar and freehand experimental knapping products from Olduvai Gorge, Tanzania. Quat. Int. 424, 58–68.

Cerling, T.E., Wynn, J.G., Andanje, S.A., Bird, M.I., Korir, D.K., Levin, N.E., Mace, W., Macharia, A.N., Quade, J., Remien, C.H., 2011. Woody cover and hominin environments in the past 6 million years. Nature 476, 51–56.

Cerling, T.E., Manthi, F.K., Mbua, E.N., Leakey, L.N., Leakey, M.G., Leakey, R.E., Brown, F.H., Grine, F.E., Hart, J.A., Kaleme, P., 2013. Stable isotope-based diet reconstructions of Turkana Basin hominins. Proc. Natl. Acad. Sci. USA 110, 10501–10506.

Cerling, T.E., Andanje, S.A., Blumenthal, S.A., Brown, F.H., Chritz, K.L., Harris, J.M., Hart, J.A., Kirera, F.M., Kaleme, P., Leakey, L.N., 2015. Dietary changes of large herbivores in the Turkana basin, Kenya from 4 to 1 Ma. Proc. Natl. Acad. Sci. USA 112, 11467–11472.

Chavaillon, J., 1976. Evidence for the technical practices of early Pleistocene hominids. Shungura formations, lower Omo valley, Ethiopia. In: Coppens, Y., Howell, F.C., Isaac, G., Leakey, R.E.F. (Eds.), Earliest Man and Environments in the Lake Rudolf Basin. University of Chicago Press, Chicago, pp. 565–573.

Çiner, A., Doğan, U., Yıldırım, C., Akçar, N., Ivy-Ochs, S., Alfimov, V., Kubik, P.W., Schlüchter, C., 2015. Quaternary uplift rates of the Central Anatolian Plateau, Turkey: Insights from cosmogenic isochron-burial nuclide dating of the Kızılırmak River terraces. Quat. Sci. Rev. 107, 81–97.

de la Torre, I., 2004. Omo revisited: Evaluating the technological skills of Pliocene hominids. Curr. Anthropol. 45, 439–465.

de la Torre, I., Mora, R., 2005. Technological Strategies in the Lower Pleistocene at Olduvai Beds I and II. Universite de Liege Press, Liege.

de la Torre, I., Mora, R., 2018. Oldowan technological behaviour at HWK EE (Olduvai Gorge, Tanzania). J. Hum. Evol. 120, 236–273.

de la Torre, I., Mora, R., Domınguez-Rodrigo, M., de Luque, L., Alcalá, L., 2003. The Oldowan industry of Peninj and its bearing on the reconstruction of the technological skills of Lower Pleistocene hominids. J. Hum. Evol. 44, 203–224.

de Lumley, H., de Lumley, M.A., Echassoux, A., Byrne, L., 2023. Fejej (FJ-1), Ethiopia. In: Beyin, A., Wright, D.K., Wilkins, J., Olszewski, D.I. (Eds.), Handbook of Pleistocene Archaeology of Africa: Hominin Behavior, Geography, and Chronology. Springer International Publishing, Cambridge, pp. 285–313.

Debénath, A., Dibble, H.L., 1994. Handbook of Paleolithic Typology: Lower and Middle Paleolithic of Europe. University of Pennsylvania Press, University of Pennsylvania Museum of Archaeology and Anthropology, Philadelphia.

Delagnes, A., Roche, H., 2005. Late Pliocene hominid knapping skills: The case of Lokalalei 2C, West Turkana, Kenya. J. Hum. Evol. 48, 435–472.

Delagnes, A., Boisserie, J.-R., Beyene, Y., Chuniaud, K., Guillemot, C., Schuster, M., 2011. Archaeological investigations in the lower Omo valley (Shungura Formation, Ethiopia): New data and perspectives. J. Hum. Evol. 61, 215.

Dibble, H.L., 1995. Middle Paleolithic scraper reduction: Background, clarification, and review of the evidence to date. J. Archaeol. Method Theory 2, 299–368.

Dibble, H.L., Holdaway, S.J., Lin, S.C., Braun, D.R., Douglass, M.J., Iovita, R., McPherron, S.P., Olszewski, D.I., Sandgathe, D., 2017. Major fallacies surrounding stone artifacts and assemblages. J. Archaeol. Method Theory 24, 813–851.

Diez-Martín, F., Sánchez, P., Domínguez-Rodrigo, M., Mabulla, A., Barba, R., 2009. Were Olduvai hominins making butchering tools or battering tools? Analysis of a recently excavated lithic assemblage from BK (Bed II, Olduvai Gorge, Tanzania). J. Anthropol. Archaeol. 28, 274–289.

Diez-Martín, F., Yustos, P.S., Domínguez-Rodrigo, M., Prendergast, M.E., 2011. An experimental study of bipolar and freehand knapping of Naibor Soit quartz from Olduvai Gorge (Tanzania). Am. Antiq. 76, 690–708.

Diez-Martín, F., Cobo-Sanchez, L., Baddeley, A., Uribelarrea, D., Mabulla, A., Baquedano, E., Domínguez-Rodrigo, M., 2021. Tracing the spatial imprint of Oldowan technological behaviors: A view from DS (Bed I, Olduvai Gorge, Tanzania). PLoS One 16, e0254603.

Diez-Martín, F., Panera, J., Maíllo-Fernández, J.M., Santonja, M., Sánchez-Yustos, P., Pérez-González, A., Duque, J., Rubio, S., Marín, J., Fraile, C., Mabulla, A., 2022. The evolution of stone tool technology at Olduvai Gorge (Tanzania): Contributions from the Olduvai paleoanthropology and paleoecology project. L'Anthropologie 126, 103000.

Ditchfield, P., Hicks, J., Plummer, T., Bishop, L.C., Potts, R., 1999. Current research on the late Pliocene and Pleistocene deposits north of Homa Mountain, southwestern Kenya. J. Hum. Evol. 36, 123–150.

Ditchfield, P.W., Whitfield, E., Vincent, T., Plummer, T., Braun, D., Deino, A., Hertel, F., Oliver, J.S., Louys, J., Bishop, L.C., 2019. Geochronology and physical context of Oldowan site formation at Kanjera South, Kenya. Geol. Mag. 156, 1190–1200.

Driscoll, K., 2011. Vein quartz in lithic traditions: An analysis based on experimental archaeology. J. Archaeol. Sci. 38, 734–745.

Fenton, C.R., Binnie, S.A., Dunai, T., Niedermann, S., 2022. The SPICE project: Calibrated cosmogenic 26Al production rates and cross-calibrated 26Al/10Be, 26Al/14C, and 26Al/21Ne ratios in quartz from the SP basalt flow, AZ, USA. Quat. Geochronol. 67, 101218.

Ferraro, J.V., Plummer, T.W., Pobiner, B.L., Oliver, J.S., Bishop, L.C., Braun, D.R., Ditchfield, P.W., Iii, J.W.S., Binetti, K.M., Jr, J.W.S., Hertel, F., Potts, R., 2013. Earliest archaeological evidence of persistent hominin carnivory. PLoS One 8, e62174.

Finestone, E.M., Braun, D.R., Plummer, T.W., Bartilol, S., Kiprono, N., 2020. Building ED-XRF datasets for sourcing rhyolite and quartzite artifacts: A case study on the Homa Peninsula, Kenya. J. Archaeol. Sci. Rep. 33, 102510.

Fisher, R.A., 1953. Dispersion on a sphere. Proc. R. Soc. Lond. AMath. Phys. Sci. 217, 295–305.

Gibbon, R.J., Pickering, T.R., Sutton, M.B., Heaton, J.L., Kuman, K., Clarke, R.J., Brain, C.K., Granger, D.E., 2014. Cosmogenic nuclide burial dating of hominin-bearing Pleistocene cave deposits at Swartkrans, South Africa. Quat. Geochronol. 24, 10–15.

Goethals, M.M., Hetzel, R., Niedermann, S., Wittmann, H., Fenton, C.R., Kubik, P.W., Christl, M., von Blanckenburg, F., 2009. An improved experimental determination of cosmogenic 10Be/21Ne and 26Al/21Ne production ratios in quartz. Earth Planet Sci. Lett. 284, 187–198.

Goldman-Neuman, T., Hovers, E., 2012. Raw material selectivity in Late Pliocene Oldowan sites in the Makaamitalu Basin, Hadar, Ethiopia. J. Hum. Evol. 62, 353–366.

Granger, D.E., 2014. Cosmogenic nuclide burial dating in archaeology and paleoanthropology. Elements 10, 369–373.

Granger, D.E., Muzikar, P.F., 2001. Dating sediment burial with in situ-produced cosmogenic nuclides: theory, techniques, and limitations. Earth Planet Sci. Lett. 188, 269–281.

Granger, D.E., Gibbon, R.J., Kuman, K., Clarke, R.J., Bruxelles, L., Caffee, M.W., 2015. New cosmogenic burial ages for Sterkfontein Member 2 *Australopithecus* and Member 5 Oldowan. Nature 522, 85–88.

Gurtov, A.N., Eren, M.I., 2014. Lower Paleolithic bipolar reduction and hominin selection of quartz at Olduvai Gorge, Tanzania: What's the connection? Quat. Int. 322, 285–291.

Harmand, S., 2009a. Raw materials and techno-economic behaviors at Oldowan and Acheulean sites in the West Turkana region, Kenya. In: Adams, B., Blades, B. (Eds.), Lithic Materials and Paleolithic Societies. Blackwell Publishing, New York, pp. 1–14.

Harmand, S., 2009b. Variability in raw material selectivity at the Late Pliocene sites of Lokalalei, West Turkana, Kenya. In: Hovers, E., Braun, D.R. (Eds.), Interdisciplinary Approaches to the Oldowan. Springer, Dordrecht, pp. 85–97.

Harmand, S., Lewis, J.E., Feibel, C.S., Lepre, C.J., Prat, S., Lenoble, A., Boës, X., Quinn, R. L., Brenet, M., Arroyo, A., 2015. 3.3-million-year-old stone tools from Lomekwi 3, West Turkana, Kenya. Nature 521, 310–315.

Herries, A.I., Martin, J.M., Leece, A.B., Adams, J.W., Boschian, G., Joannes-Boyau, R., Edwards, T.R., Mallett, T., Massey, J., Murszewski, A., 2020. Contemporaneity of *Australopithecus, Paranthropus*, and early *Homo erectus* in South Africa. Science 368, eaaw7293.

Hlubik, S., Cutts, R., Braun, D.R., Berna, F., Feibel, C.S., Harris, J.W., 2019. Hominin fire use in the Okote member at Koobi Fora, Kenya: New evidence for the old debate. J. Hum. Evol. 133, 214–229.

Hovers, E., 2009. Learning from mistakes: Flaking accidents and knapping skills in the assemblage of AL 894 (Hadar, Ethiopia). In: Schick, K., Toth, N. (Eds.), The Cutting Edge: New Approaches to the Archaeology of Human Origins. Stone Age Institute Press, Gosport, pp. 137–150.

Isaac, G.L., Behrensmeyer, A.K., 1997. Geological context and palaeoenvironments. In: Isaac, G.L. (Ed.), Koobi Fora Research Project 5. Clarendon Press, Oxford, pp. 12–70.

Isaac, G.L., Harris, J.W.K., Kroll, E.M., 1997. Plio-Pleistocene Archeology. The stone artifact assemblages: A comparative study. In: Isaac, G., Isaac, B. (Eds.), Koobi Fora Research Project, Volume 5: Plio- Pleistocene Archaeology. Clarendon Press, Oxford, pp. 262–299.

Kibunjia, M., 1994. Pliocene archaeological occurrences in the Lake Turkana basin. J. Hum. Evol. 27, 159–171.

Kimura, Y., 1999. Tool-using strategies by early hominids at bed II, Olduvai Gorge, Tanzania. J. Hum. Evol. 37, 807–831.

Kimura, Y., 2002. Examining time trends in the Oldowan technology at Beds I and II, Olduvai Gorge. J. Hum. Evol. 43, 291–321.

Kingston, J.D., 2007. Shifting adaptive landscapes: Progress and challenges in reconstructing early hominid environments. Am. J. Phys. Anthropol. 134, 20–58.

Kirschvink, J.L., 1980. The least-squares line and plane and the analysis of palaeomagnetic data. Geophys. J. Int. 62, 699–718.

Kuhn, S.L., 2004. Upper Paleolithic raw material economies at Üçağızlı cave, Turkey. J. Anthropol. Archaeol. 23, 431–448.

Lê, S., Josse, J., Husson, F., 2008. FactoMineR: An R package for multivariate analysis. J. Stat. Softw. 25, 1–18.

Le Bas, M.J., 1977. Carbonatite-Nephelinite Volcanism: an African Case History. Wiley, London.

Leakey, M.D., 1971. Olduvai Gorge: Volume 3, Excavations in Beds I and II, vol. 3. Cambridge University Press, Cambridge, pp. 1960–1963.

Lemorini, C., Plummer, T.W., Braun, D.R., Crittenden, A.N., Ditchfield, P.W., Bishop, L. C., Hertel, F., Oliver, J.S., Marlowe, F.W., Schoeninger, M.J., 2014. Old stones' song: Use-wear experiments and analysis of the Oldowan quartz and quartzite assemblage from Kanjera South (Kenya). J. Hum. Evol. 72, 10–25.

Lemorini, C., Bishop, L.C., Plummer, T.W., Braun, D.R., Ditchfield, P.W., Oliver, J.S., 2019. Old stones' song—second verse: Use-wear analysis of rhyolite and fenetized andesite artifacts from the Oldowan industry of Kanjera South, Kenya. Archaeol. Anthropol. Sci. 11, 4729–4754.

Levin, N.E., Quade, J., Simpson, S.W., Semaw, S., Rogers, M., 2004. Isotopic evidence for Plio–Pleistocene environmental change at Gona, Ethiopia. Earth Planet Sci. Lett. 219, 93–110.

Levin, N.E., Brown, F.H., Behrensmeyer, A.K., Bobe, R., Cerling, T.E., 2011. Paleosol carbonates from the Omo Group: Isotopic records of local and regional environmental change in East Africa. Palaeogeogr. Palaeoclimatol. Palaeoecol. 307, 75–89.

Levin, N.E., Haile-Selassie, Y., Frost, S.R., Saylor, B.Z., 2015. Dietary change among hominins and cercopithecids in Ethiopia during the early Pliocene. Proc. Natl. Acad. Sci. U.S.A. 112, 12304–12309.

Liu, X., Shen, G., Tu, H., Lu, C., Granger, D.E., 2015. Initial 26Al/10Be burial dating of the hominin site Bailong cave in Hubei Province, central China. Quat. Int. 389, 235–240.

Ludwig, B.V., 1999. A technological reassessment of East African Plio-Pleistocene lithic artifact assemblages. Ph.D. Dissertation, Rutgers University.

Mackay, A., 2008. A method for estimating edge length from flake dimensions: Use and implications for technological change in the southern African MSA. J. Archaeol. Sci. 35, 614–622.

Mercader, J., Akuku, P., Boivin, N., Bugumba, R., Bushozi, P., Camacho, A., Carter, T., Clarke, S., Cueva-Temprana, A., Durkin, P., Favreau, J., 2021. Earliest Olduvai hominins exploited unstable environments~ 2 million years ago. Nat. Commun. 12, 1–15.

Miall, A.D., 2013. The Geology of Fluvial Deposits: Sedimentary Facies, Basin Analysis, and Petroleum Geology. Springer, New York.

Ogg, J.G., 2020. Geomagnetic polarity time scaleGradstein, F.M., Ogg, J.G., Smith, A.G., Ogg, G.M. (Eds.), In: Geologic Time Scale 2020, Volume 1. Elsevier, Amsterdam, pp. 159–192.

Oliver, J.S., Plummer, T.W., Hertel, F., Bishop, L.C., 2019. Bovid mortality patterns from Kanjera South, Homa Peninsula, Kenya and FLK-Zinj, Olduvai Gorge, Tanzania: Evidence for habitat mediated variability in Oldowan hominin hunting and scavenging behavior. J. Hum. Evol. 131, 61–75.

Parkinson, J.A., Plummer, T.W., Oliver, J.S., Bishop, L.C., 2022. Meat on the menu: GIS spatial distribution analysis of bone surface damage indicates that Oldowan hominins at Kanjera South, Kenya had early access to carcasses. Quat. Sci. Rev. 277, 107314.

Plummer, T., 2004. Flaked stones and old bones: Biological and cultural evolution at the dawn of technology. Am. J. Phys. Anthropol. 125, 118–164.

Plummer, T., Bishop, L.C., Ditchfield, P., Hicks, J., 1999. Research on Late Pliocene Oldowan sites at Kanjera South, Kenya. J. Hum. Evol. 36, 151–170.

Plummer, T.W., Bishop, L.C., Ditchfield, P.W., Ferraro, J.V., Kingston, J.D., Hertel, F., Braun, D.R., 2009a. The environmental context of Oldowan hominin activities at Kanjera South, Kenya. In: Hovers, E., Braun, D.R. (Eds.), Interdisciplinary Approaches to the Oldowan. Springer, New York, pp. 149–160.

Plummer, T.W., Ditchfield, P.W., Bishop, L.C., Kingston, J.D., Ferraro, J.V., Braun, D.R., Hertel, F., Potts, R., 2009b. Oldest evidence of toolmaking hominins in a grassland-dominated ecosystem. PLoS One 4, e7199.

Plummer, T.W., Bishop, L.C., 2016. Oldowan hominin behavior and ecology at Kanjera South, Kenya. J. Anthropol. Sci. 94, 29–40.

Plummer, T.W., Finestone, E.M., 2018. Archeological sites from 2.6-2.0 Ma: Toward a deeper understanding of the early Oldowan. In: Schwartz, J.H. (Ed.), Rethinking Human Evolution. MIT Press, Cambridge, pp. 267–296.

Plummer, T.W., Oliver, J.S., Finestone, E.M., Ditchfield, P.W., Bishop, L.C., Blumenthal, S.A., Lemorini, C., Caricola, I., Bailey, S.E., Herries, A.I.R., Parkinson, J. A., Whitfield, E., Hertel, F., Kinyanjui, R.N., Vincent, T.H., Li, Y., Louys, J., Frost, S. R., Braun, D.R., Reeves, J.S., Early, E.D.G., Onyango, B., Lamela-Lopez, R., Forrest, F. L., He, H., Lane, T.P., Frouin, M., Nomade, S., Wilson, E.P., Bartilol, S.K., Rotich, N. K., Potts, R., 2023. Expanded geographic distribution and dietary strategies of the earliest Oldowan hominins and *Paranthropus*. Science 379, 561–566.

Polissar, P.J., Rose, C., Uno, K.T., Phelps, S.R., deMenocal, P., 2019. Synchronous rise of African C4 ecosystems 10 million years ago in the absence of aridification. Nat. Geosci. 12, 657–660.

Pontzer, H., 2012. Ecological energetics in early *Homo*. Curr. Anthropol. 53, S346–S358.

Pontzer, H., Brown, M.H., Raichlen, D.A., Dunsworth, H., Hare, B., Walker, K., Luke, A., Dugas, L.R., Durazo-Arvizu, R., Schoeller, D., 2016. Metabolic acceleration and the evolution of human brain size and life history. Nature 533, 390–392.

Potts, R., 2007. Environmental hypotheses of Pliocene human evolution. In: Bobe, R., Alemseged, Z., Behrensmeyer, A.K. (Eds.), Hominin Environments in the East African Pliocene: An Assessment of the Faunal Evidence. Springer, Dordrecht, pp. 25–49.

Potts, R., Faith, J.T., 2015. Alternating high and low climate variability: The context of natural selection and speciation in Plio-Pleistocene hominin evolution. J. Hum. Evol. 87, 5–20.

Quade, J., Levin, N., Semaw, S., Stout, D., Renne, P., Rogers, M., Simpson, S., 2004. Paleoenvironments of the earliest stone toolmakers, Gona, Ethiopia. Geol. Soc. Am. Bull. 116, 1529–1544.

Quinn, R.L., Lepre, C.J., Feibel, C.S., Wright, J.D., Mortlock, R.A., Harmand, S., Brugal, J.-P., Roche, H., 2013. Pedogenic carbonate stable isotopic evidence for wooded habitat preference of early Pleistocene tool makers in the Turkana Basin. J. Hum. Evol. 65, 65–78.

R Core Team, 2022. R: A language and environment for statistical computing. R Foundation for Statistical Computing, Vienna.

Reeves, J.S., Braun, D.R., Finestone, E.M., Plummer, T.W., 2021. Ecological perspectives on technological diversity at Kanjera South. J. Hum. Evol. 158, 103029.

Robinson, J.R., Rowan, J., Campisano, C.J., Wynn, J.G., Reed, K.E., 2017. Late Pliocene environmental change during the transition from *Australopithecus* to *Homo*. Nat. Ecol. Evol. 1, 1–7.

Roche, H., Delagnes, A., Brugal, J.-P., Feibel, C., Kibunjia, M., Mourre, V., Texier, P.-J., 1999. Early hominid stone tool production and technical skill 2.34 Myr ago in West Turkana, Kenya. Nature 399, 57–60.

Roche, H., Blumenschine, R.J., Shea, J.J., 2009. Origins and adaptations of early *Homo*: What archeology tells us. In: Grine, F.E., Fleagle, J.G., Leakey, R.E. (Eds.), The First Humans–Origin and Early Evolution of the Genus *Homo*: Contributions from the Third Stony Brook Human Evolution Symposium and Workshop October 3–October 7, 2006. Springer, New York, pp. 135–147.

Rodés, A., 2021. The NUNAtak Ice Thinning (NUNAIT) calculator for cosmonuclide elevation profiles. Geosciences 11, 362.

Rogers, M.J., Harris, J.W., Feibel, C.S., 1994. Changing patterns of land use by Plio-Pleistocene hominids in the lake Turkana basin. J. Hum. Evol. 27, 139–158.

Rogers, M.J., Semaw, S., 2009. From nothing to something: The appearance and context of the earliest archaeological record. In: Camps, M., Chauhan, P. (Eds.), Sourcebook of Paleolithic Transitions. Springer, New York, pp. 155–171.

Roth, B.J., Dibble, H.L., 1998. Production and transport of blanks and tools at the French Middle Paleolithic site of Combe-Capelle Bas. Am. Antiq. 63, 47–62.

Saggerson, E.P., 1952. Geology of the Kisumu District. Geol. Surv. Kenya Rep. 21, 1–86.

Schick, K., 1987. Modeling the formation of early stone age artifact concentrations. J. Hum. Evol. 16, 789–807.

Semaw, S., 2000. The world's oldest stone artefacts from Gona, Ethiopia: Their implications for understanding stone technology and patterns of human evolution between 2·6–1·5 million years ago. J. Archaeol. Sci. 27, 1197–1214.

Semaw, S., Renne, P., Harris, J.W., Feibel, C.S., Bernor, R.L., Fesseha, N., Mowbray, K., 1997. 2.5-million-year-old stone tools from Gona, Ethiopia. Nature 385, 333–336.

Semaw, S., Rogers, M.J., Quade, J., Renne, P.R., Butler, R.F., Dominguez-Rodrigo, M., Stout, D., Hart, W.S., Pickering, T., Simpson, S.W., 2003. 2.6-Million-year-old stone tools and associated bones from OGS-6 and OGS-7, Gona, Afar, Ethiopia. J. Hum. Evol. 45, 169–177.

Sikes, N.E., 1994. Early hominid habitat preferences in East Africa: Paleosol carbon isotopic evidence. J. Hum. Evol. 27, 25–45.

Sikes, N.E., Ashley, G.M., 2007. Stable isotopes of pedogenic carbonates as indicators of paleoecology in the Plio-Pleistocene (upper Bed I), western margin of the Olduvai Basin, Tanzania. J. Hum. Evol. 53, 574–594.

Singer, B.S., 2014. A Quaternary geomagnetic instability time scale. Quat. Geochronol. 21, 29–52.

Stout, D., Quade, J., Semaw, S., Rogers, M.J., Levin, N.E., 2005. Raw material selectivity of the earliest stone toolmakers at Gona, Afar, Ethiopia. J. Hum. Evol. 48, 365–380.

Stout, D., Semaw, S., Rogers, M.J., Cauche, D., 2010. Technological variation in the earliest Oldowan from Gona, Afar, Ethiopia. J. Hum. Evol. 58, 474–491.

Susman, R.L., 1988. Hand of *Paranthropus robustus* from member 1, Swartkrans: Fossil evidence for tool behavior. Science 240, 781–784.

Susman, R.L., 1991. Who made the Oldowan tools? Fossil evidence for tool behavior in Plio-Pleistocene hominids. J. Anthropol. Res. 47, 129–151.

Tallavaara, M., Manninen, M.A., Hertell, E., Rankama, T., 2010. How flakes shatter: A critical evaluation of quartz fracture analysis. J. Archaeol. Sci. 37, 2442–2448.

Tarriño, A., Ábalos, B., Puelles, P., Eguiluz, L., Díez-Martín, F., 2023. The crystalline quartz-rich raw material from Olduvai Gorge (Tanzania): Why is it called quartzite when it should be called quartz? Archaeol. Anthropol. Sci 15, 78.

Toth, N.P., 1982. The stone technologies of early hominids at Koobi Fora, Kenya: An experimental approach. Ph.D. Dissertation, University of California, Berkeley.

Toth, N., 1987. Behavioral inferences from early stone artifact assemblages: An experimental model. J. Hum. Evol. 16, 763–787.

Toth, N., 1997. The artefact assemblages in the light of experimental studies. In: Isaac, G. L. (Ed.), Koobi Fora Research Project 5. Clarendon Press, Oxford, pp. 363–401.

Toth, N., Schick, K., 2018. An overview of the cognitive implications of the Oldowan Industrial Complex. Azania 53, 3–39.

Uno, K.T., Polissar, P.J., Jackson, K.E., deMenocal, P.B., 2016. Neogene biomarker record of vegetation change in eastern Africa. Proc. Natl. Acad. Sci. USA 113, 6355–6363.

Uno, K.T., Rivals, F., Bibi, F., Pante, M., Njau, J., de la Torre, I., 2018. Large mammal diets and paleoecology across the Oldowan–Acheulean transition at Olduvai Gorge, Tanzania from stable isotope and tooth wear analyses. J. Hum. Evol. 120, 76–91.

Wheeler, P.E., 1994. The thermoregulatory advantages of heat storage and shade-seeking behaviour to hominids foraging in equatorial savannah environments. J. Hum. Evol. 26, 339–350.

Wood, B., 1997. The oldest whodunnit in the world. Nature 385, 292–293.

Wrangham, R.W., Carmody, R.N., 2010. Human adaptation to the control of fire. Evol. Anthropol. 199, 197–199.

Wynn, J.G., 2007. Carbon isotope fractionation during decomposition of organic matter in soils and paleosols: Implications for paleoecological interpretations of paleosols. Palaeogeogr. Palaeoclimatol. Palaeoecol. 251, 437–448.